DOI: 10.1002/chem.200600689

Synthesis, Fluorescence, and Two-Photon Absorption of a Series of Elongated Rodlike and Banana-Shaped Quadrupolar Fluorophores: A Comprehensive Study of Structure–Property Relationships

Olivier Mongin,* Laurent Porrès, Marina Charlot, Claudine Katan, and Mireille Blanchard-Desce*[a]

Abstract: An extensive series of push–push and pull–pull derivatives was prepared from the symmetrical functionalization of an ambivalent core with conjugated rods made from arylene–vinylene or arylene–ethynylene building blocks, bearing different acceptor or donor end-groups. Their absorption and photoluminescence, as well as their two-photon-absorption (TPA) properties in the near infrared (NIR) region, were systematically investigated to derive structure–property relationships and to lay the guidelines for both spectral tuning and amplification of molecular TPA in the target region. Whatever the nature of the core or of the connectors, push–push systems were found to be more efficient than pull–pull systems, and planarization of the core (fluorene versus biphenyl) always leads to an increase in the TPA cross sections. In contrast, increasing the conjugation length as well as replacement of a phenylene moiety by a thienylene moiety in the conjugated rods *did not* necessarily lead to increased TPA responses. The present study also demonstrated that the topology of the conjugated rods can dramatically influence the TPA properties. This is of particular interest in terms of molecular engineering for specific applications, as both TPA properties and photoluminescence characteristics can be considerably affected. Thus, it becomes possible to optimize the transparency/TPA and fluorescence/TPA efficiency tradeoffs for optical limiting in the red-NIR region (700–900 nm) and for two-photon-excited fluorescence (TPEF) microscopy applications, respectively.

Keywords: chromophores · fluorescence · nonlinear optics · photoluminescence · two-photon absorption

Introduction

Molecular two-photon absorption (TPA) has attracted growing interest over recent years owing to its applications in various fields such as spectroscopy,[1,2] three-dimensional optical data storage,[3–7] microfabrication,[8–11] laser up-conversion,[12,13] high-resolution three-dimensional imaging of biological systems,[14–17] and photodynamic therapy.[18] Among these, two-photon-excited fluorescence (TPEF) has gained widespread popularity in the biology community and has given rise to the technique of two-photon laser scanning fluorescence microscopy,[14–16] which enables, for instance, in vivo imaging of calcium dynamics[17,19–21] or intracellular zinc.[22,23] Use of a two-photon-excitation process (i.e., a nonlinear process involving the *simultaneous* absorption of two photons) instead of a conventional one-photon excitation actually offers a number of advantages. These include the ability for a highly confined excitation and intrinsic three-dimensional resolution in microscopic imaging. Moreover, by replacing one-photon excitation in the UV-visible blue region by two-photon excitation in the visible red-NIR region (typically 700–1200 nm), TPEF offers the advantage of imaging at an increased penetration depth in tissues (owing in particular to a reduction of scattering losses) with reduced photodamage, as well as improved signal-to-noise ratio (owing to reduced background fluorescence). The fast development of TPEF microscopy has triggered the search for novel fluorophores specifically engineered for TPEF. Fluorophores with TPA cross sections many orders of mag-

[a] Dr. O. Mongin, Dr. L. Porrès, Dr. M. Charlot, Dr. C. Katan, Dr. M. Blanchard-Desce
Synthèse et ElectroSynthèse Organiques (CNRS, UMR 6510)
Institut de Chimie, Université de Rennes 1
Campus Scientifique de Beaulieu, Bât 10A
35042 Rennes Cedex (France)
Fax: (+33) 223-236-955
E-mail: olivier.mongin@univ-rennes1.fr
mireille.blanchard-desce@univ-rennes1.fr

Supporting information for this article is available on the WWW under http://www.chemeurj.org/ or from the author.

 © 2007 Wiley-VCH Verlag GmbH & Co. KGaA, Weinheim

nitude larger than endogenous fluorophores (such as fluorescent amino acids, flavins)[24–26] are attractive for reducing background fluorescence by *selective* two-photon-excitation of TPEF probes. In addition, TPEF fluorophores with both broad and intense TPA bands are also of interest because of the versatility they offer in terms of excitation sources (insofar as costly, tunable short-pulse lasers can be replaced by less-expensive, nontunable laser sources).

Multiphoton absorption has also attracted considerable attention for optical limiting,[27–39] focusing mainly on optical limiting in the visible region aiming at eye protection.[37–39] Although a number of multiphoton chromophores have been designed and studied in this context, only scarce effort has been dedicated to the protection of near infrared (NIR) detectors typically working in the 700–900 nm region. Thus, chromophores combining full transparency and strong multiphoton absorptivities (such as overlapping of strong two-photon and excited-state absorptions) in that spectral range are required.

Within this context, we have implemented a molecular-engineering approach towards elongated rodlike or banana-shaped fluorophores with enhanced TPA cross sections (σ_2) in the target spectral window (i.e., 700–1000 nm).[40] A high fluorescence quantum yield (Φ) is required for TPEF applications, whereas a full linear transparency is required for optical-limiting applications. Here, we describe and discuss their molecular design, synthesis, photophysical and TPA properties. A wide scope of molecules was prepared and investigated to derive structure–property relationships and to lay the guidelines for both spectral tuning of both absorption and fluorescence and amplification of molecular TPA.

By following the route for molecular TPA optimization proposed by Marder and collaborators,[41,42] we focused on the optimization of quasi-one-dimensional quadrupolar systems, that is, symmetrical conjugated molecules bearing two electron-releasing (D) or electron-withdrawing (A) end-groups.[40,43–45] Indeed, quadrupolar systems[27,30,35,39–79] have been found to be more efficient than push–pull systems[13,28,46,47,56,64,68,80–88] in terms of TPA, in particular for multiphoton-based optical-limiting applications.[27,30,39] Such derivatives can display very large TPA cross sections in connection with a quadrupolar intramolecular charge transfer taking place between the ends and the center of the molecules.[42] Very large σ_2 values have been obtained with DAAD, ADDA, DADAD, DDADD··· systems having strong D and A moieties, but often at the cost of reduced fluorescence quantum yield and/or pronounced red-shift of the one-photon-absorption band.[41,77] In this context, our purpose was the design of optimized systems displaying enhanced σ_2 values in the red-NIR region (700–1000 nm), while maintaining high fluorescence quantum yields. Our strategy, founded on a three-VB-state model,[89–91] was based on the push–push or pull–pull functionalization of a semirigid, conjugated system.[40,43–45]

The structure was built from the symmetrical grafting, onto a conjugated core, of two elongated conjugated rods bearing either a D or A end-group (Figure 1). The central building blocks were selected as more or less rigid units that may assist quadrupolar intramolecular charge transfer by acting either as a (weak) donor or acceptor core. We selected biphenyl (BP) or fluorene (Fl) central units, which allow the tuning of the electronic delocalization along the conjugated backbone in the ground state by modulation of the twist angle between the two halves of the molecules.[40] It should be noted that the fluorene building block was successfully used in the design of both dipolar[46,83] and quadrupolar systems with large multiphoton absorption,[40,59,69] owing to the planarity it provides. Conjugated rods built

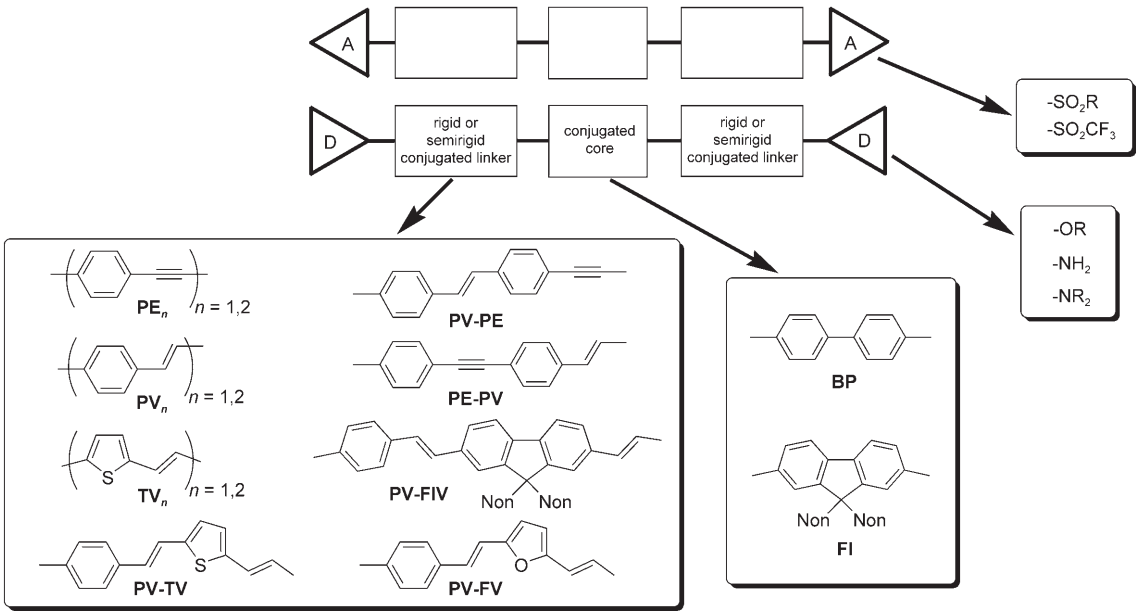

Figure 1. Molecular engineering of pull–pull and push–push fluorophores designed for TPEF (Non = nonyl).

 © 2007 Wiley-VCH Verlag GmbH & Co. KGaA, Weinheim

from arylene–ethynylene and/or arylene–vinylene oligomers were investigated to maintain fluorescence and to modulate the electronic communication between the end-groups and the core of the molecules. The aim of these systematic structural variations was both to derive comprehensive structure–TPA relationships and to ascertain the appropriate combination of core, linker (double versus triple bond), and connector (phenylene P, thienylene T, furylene F, fluorenylene Fl) moieties for optimized TPA/luminescence and/or TPA/transparency properties. Long alkyl chains were grafted onto the peripheral groups and/or onto the core to obtain highly soluble derivatives, which are required for optical-limiting applications. Moreover, the central nonyl chains on the fluorenyl core were intended to hinder π stacking and aggregation processes that are detrimental to TPA[79] and photoluminescence properties.

Results and Discussion

Synthesis: The assembly of cores, linkers, and end-groups was performed by means of Sonogashira or Heck couplings and Wittig or Horner–Wadsworth–Emmons condensations. Amino (**1a**) and dialkylamino (**1b**)[92] moieties bearing an iodo group were used as electron-releasing building blocks, and **1b** was also converted to the extended rigid moieties **2a** and **2b** in three-step sequences: 1) palladium(II)-catalyzed reaction with 2-methyl-3-butyn-2-ol, 2) base-promoted deprotection, and 3) cross-coupling with 1,4-diiodobenzene and 4-bromobenzaldehyde, respectively (Scheme 1). Other electron-donating dialkylamino building blocks were prepared, bearing either a formyl (**1e**)[93] or a phosphonium (**3a–c**)[94] group. Phosphonium salts **3b** and **3c** were also converted to the semirigid stilbene rods **4b** and **4a**, respectively, through their Wittig condensation with terephthalaldehyde mono(diethylacetal) and 4-iodobenzaldehyde, respectively. The furylene–vinylene- and thienylene–vinylene-containing building blocks **6a–c** were obtained by reaction of 2,5-furanedicarboxaldehyde monoacetal (**5a**)[95] or 2,5-thiophenedicarboxaldehyde monoacetal (**5b**)[96] with phosphonium salts **3b** or **3c**, followed by acidic hydrolysis of the intermediate acetals (Scheme 1).

The electron-withdrawing alkylsulfone **8a** was prepared by oxidation of thioether **7a**,[97] and the trifluoromethylsulfone **8d** was obtained from **7b** in a three-step sequence, involving oxidation, palladium(II)-catalyzed reaction with ethynyltrimethylsilane, and cleavage of the trimethylsilyl group. Phosphonates **9a**[98] and **9b**, as well as phenylene–vinylene-extended phosphonate **11**,[99] were also used as electron-withdrawing moieties. The halogen-bearing sulfone **10** was obtained from a Horner–Wadsworth–Emmons condensation between **9b** and 4-iodobenzaldehyde (Scheme 2).

The synthesis of the biphenyl-cored fluorophores **13a**, **13b**, and **14** was achieved by means of a double Sonogashira coupling of **12**[100] with **1b**, **2a**, and **4a**, respectively (Scheme 3). Bisphosphonate **15b** (prepared by Michaelis–Arbusov reaction of 4,4′-bis(bromomethyl)-1,1′-biphenyl

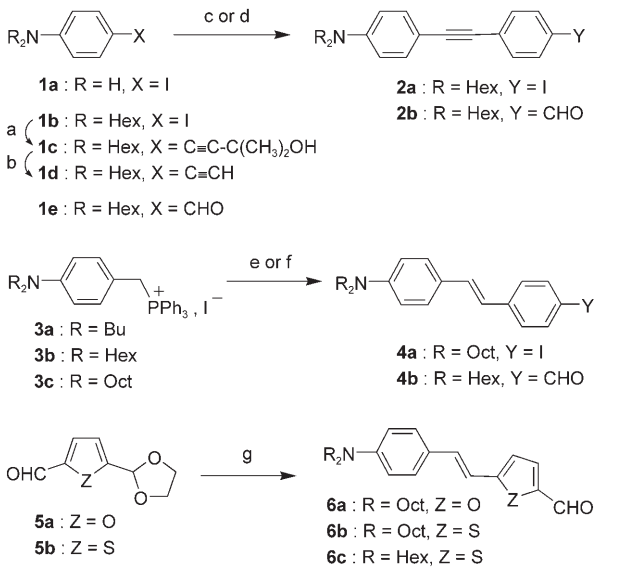

Scheme 1. a) 2-methyl-3-butyn-2-ol, $[Pd(PPh_3)_2Cl_2]$, CuI, Et_3N, 40 °C, 12 h (82 %); b) NaOH, toluene/*i*PrOH, reflux, 1 h (87 %); c) **1d** (1 equiv), 1,4-diiodobenzene (3 equiv), $[Pd(PPh_3)_2Cl_2]$, CuI, toluene/Et_3N, 30 °C, 6 h (71 % of **2a**); d) **1d** (1 equiv), 4-bromobenzaldehyde (1.2 equiv), $[Pd(PPh_3)_2Cl_2]$, CuI, toluene/Et_3N, 40 °C, 15 h (74 % of **2b**); e) **3c**, 4-iodobenzaldehyde, *t*BuOK, CH_2Cl_2, 20 °C, 5 h, then I_2 cat., *hν* (85 % of **4a**); f) **3b**, terephthalaldehyde mono(diethylacetal), *t*BuOK, CH_2Cl_2, 20 °C, 24 h; HCl, 20 °C, 1 h; I_2 cat., *hν* (84 % of **4b**); g) **3b** or **3c**, conditions as in (f) (95 % of **6a**, 79 % of **6b**, 85 % of **6c**). Bu = butyl, Hex = hexyl; Oct = octyl.

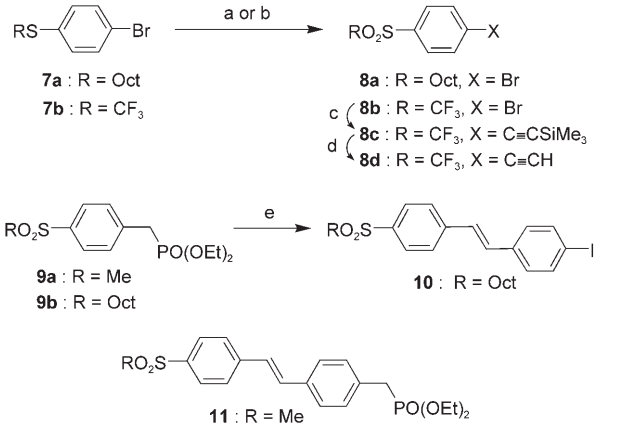

Scheme 2. a) **7a**, H_2O_2, $Na_2WO_4{\cdot}2H_2O$ cat., EtOH, reflux, 1 h (93 % of **8a**); b) **7b**, H_2O_2, AcOH, reflux, 3 h (89 % of **8b**); c) HC≡$CSiMe_3$, $[Pd(PPh_3)_2Cl_2]$, CuI, Et_3N, 40 °C, 3 h (88 %); d) tetrabutyl ammonium fluoride (TBAF), THF (64 %); e) **9b**, 4-iodobenzaldehyde, NaH, THF, 20 °C, 15 h (61 %).

(**15a**)[101] with triethylphosphite) was used to prepare the other biphenyl-cored fluorophores **16a**, **16b**, **17a**, and **17b**, by condensation with aldehydes **1e**, **2b**, **6a**, and **6c**, respectively (Scheme 3).

The fluorene core **18d** was obtained from 9,9-dinonylfluorene (**18a**) in a three-step sequence: 1) diiodination, 2) cross-coupling with 2-methyl-3-butyn-2-ol, and 3) base-promoted deprotection (Scheme 4). Double Sonogashira coupling of **18d** with **1b**, **2a**, and **4a** afforded push–push

 © 2007 Wiley-VCH Verlag GmbH & Co. KGaA, Weinheim

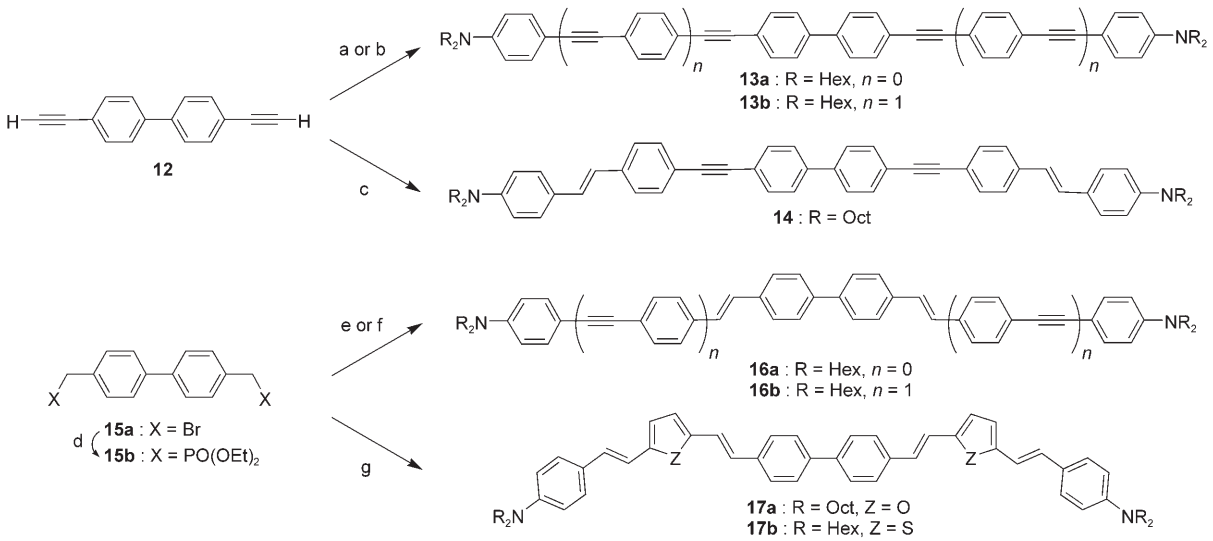

Scheme 3. a) **1b** (2.3 equiv), $[Pd(PPh_3)_2Cl_2]$, CuI, toluene/Et_3N, 20 °C, 2 h (84 % of **13a**); b) **2a**, conditions as in (a) (86 % of **13b**); c) **4a**, conditions as in (a), 3.5 h (81 %); d) $P(OEt)_3$, toluene, reflux, 60 h (86 %); e) **1e** (2 equiv), NaH, THF, 20 °C, 20 h, then reflux, 4 h (70 % of **16a**); f) **2b** (2.3 equiv), NaH, THF, [18]crown-6 cat., 40 °C, 3 h (84 % of **16b**); g) **6a** or **6c** (2.1 equiv), NaH, THF, 20 °C, 16–19 h (80 % of **17a**, 64 % of **17b**).

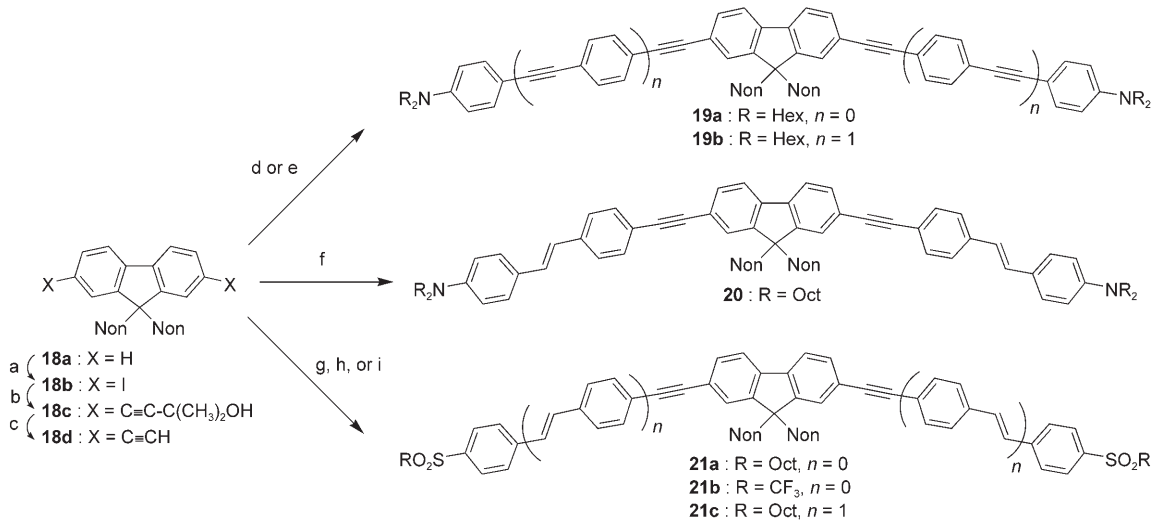

Scheme 4. a) I_2, H_5IO_6, AcOH, H_2SO_4, H_2O, 75 °C, 2 h (69 %); b) 2-methyl-3-butyn-2-ol, $[Pd(PPh_3)_2Cl_2]$, CuI, Et_3N, 20 °C, 16 h (72 %); c) KOH, toluene/*i*PrOH, reflux, 0.5 h (88 %); d) **1b** (2.4 equiv), $[Pd(PPh_3)_2Cl_2]$, CuI, toluene/Et_3N, 20 °C, 3 h (45 % of **19a**); e) **2a**, conditions as in (d), 20 h (82 % of **19b**); f) **4a**, conditions as in (d), 15 h (83 %); g) **8a**, conditions as in (d), 45 °C, 6 h (84 % of **21a**); h) **18b**, **8d** (2.5 equiv), conditions as in (d), 40 °C, 14 h (60 % of **21b**); i) **10**, conditions as in (d), 35 °C, 14 h (87 % of **21c**).

molecules **19a**, **19b**, and **20**, respectively, whereas reaction with **8a** and **10** gave pull–pull molecules **21a** and **21c**, respectively. The bistrifluoromethylsulfone **21b** was obtained by reacting the diiodo-fluorene core **18b** and the alkyne **8d** (Scheme 4).

The bisaldehyde core **22b** was also obtained from 9,9-dinonylfluorene (**18a**), by successive dibromination, double bromine–lithium exchange, and formylation reactions (Scheme 5). Wittig condensation of bisaldehyde **22b** with two equivalents of 4-(methoxybenzyl)triphenylphosphonium bromide gave (after isomerization with a catalytic amount of iodine under illumination) fluorophore **23**, whereas the same reaction with one single equivalent of phosphonium salt **3a** lead to the formation of fluorophore **24** together with the new extended building block **25**. Vinylic bissulfones **26a** and **26b** were synthesized by a double Horner–Wadsworth–Emmons condensation of the same bisaldehyde **22b** with phosphonates **9a** and **11**, respectively (Scheme 5).

The bisvinyl fluorene core **27**, obtained by condensation of **22b** with methyltriphenylphosphonium iodide, was reacted with 4-iodoaniline **1a** to afford fluorophore **28**, by means of a double Heck-type coupling under Jeffery's[102] conditions (Scheme 6).

Conversion of **22b** to the fluorenebisphosphonate **29c** was achieved in a three-step sequence (reduction, bromination, and Michaelis–Arbusov reaction). Finally, this new fluorene

 © 2007 Wiley-VCH Verlag GmbH & Co. KGaA, Weinheim

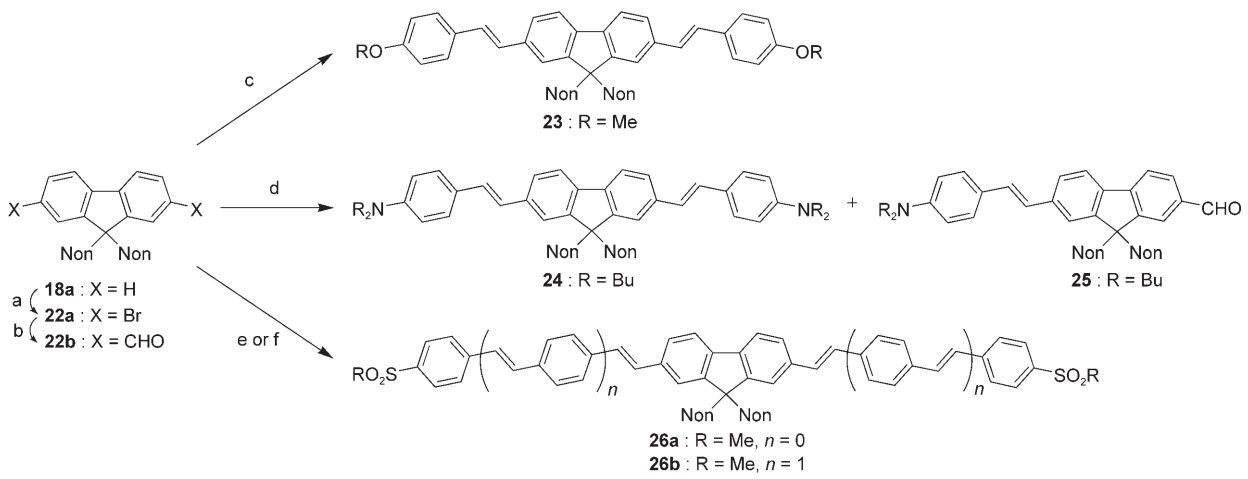

Scheme 5. a) Br_2 (2 equiv), CH_2Cl_2, 20 °C, 15 h (97 %); b) *n*BuLi, benzene, 60 °C, 4 h, then *N*-formylpiperidine, 20 °C, 14 h (48 %); c) 4-(methoxybenzyl)-triphenylphosphonium bromide (2.2 equiv), *t*BuOK, CH_2Cl_2, 20 °C, 48 h, then I_2 cat., *hν* (75 %); d) **3a** (1.0 equiv), *t*BuOK, CH_2Cl_2, 20 °C, 16 h, then I_2 cat., *hν* (12 % of **24**, 59 % of **25**); e) **9a** (2.2 equiv), NaH, THF, 20 °C, 16 h (95 % of **26a**); f) **11**, conditions as in (e) (63 % of **26b**).

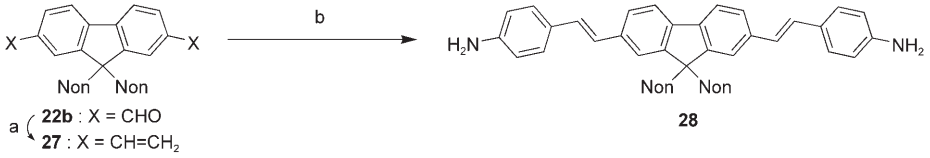

Scheme 6. a) Methyltriphenylphosphonium iodide (2.5 equiv), NaH, THF, 20 °C, 48 h (63 %); b) **1a** (2.5 equiv),[$Pd(OAc)_2$], PPh_3, nBu_4NCl, K_2CO_3, DMF, 90 °C, 22 h (56 %).

core was reacted with aldehydes **4b**, **6b**, and **25** in the presence of sodium hydride to give phenylene–vinylene-linked fluorophore **30**, its thienylene–vinylene analogue **31**, and the trimeric fluorenylene–vinylene **32**, respectively (Scheme 7).

Finally, the bisaldehyde core **22b** and its thienylene–vinylene-extended analogue **33**, obtained by reaction of bisphosphonate **29c** with **5b**, afforded fluorophores **34a** and **34b**, respectively, from double Wittig condensations with {[5-(1-piperidinyl)-2-thienyl]-methyl}triphenylphosphonium iodide (Scheme 8).

All new fluorophores were fully characterized by NMR spectroscopy, HRMS, and/or elemental analysis. The ^1H and ^{13}C NMR spectra confirm their high symmetry. In addition, their all-*E* stereochemistry was derived from the values of the ^3J coupling constants between vinylic protons ($J \sim 16$ Hz). All the dinonylfluorene derivatives are extremely soluble in chlorinated solvents (typically higher than 500 $g\,L^{-1}$) as well as in THF and toluene, whereas the extended biphenyl fluorophores (**13b**, **14**, **16b**) exhibit much lower solubilities (1–5 $g\,L^{-1}$). Long alkyl chains located on the central cores are more efficient in increasing the solubility than those located on the peripheral groups.

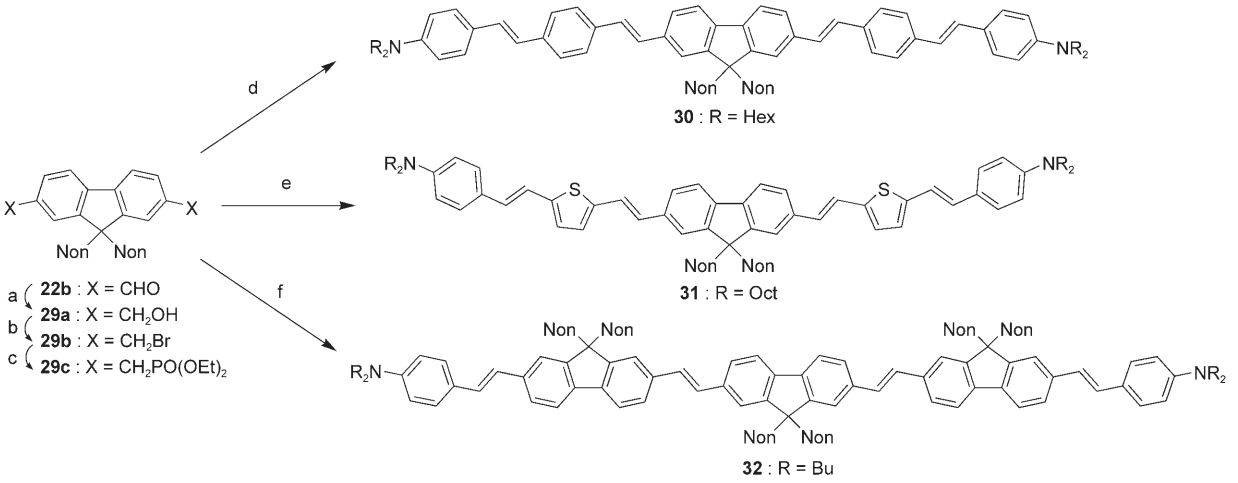

Scheme 7. a) KBH_4, $EtOH/CH_2Cl_2$, 20 °C, 14 h (97 %); b) concd HBr, reflux, 3 h (90 %); c) $P(OEt)_3$, reflux, 60 h (62 %); d) **4b** (2.2 equiv), NaH, THF, 20 °C, 20 h (53 %); e) **6b** (2.5 equiv), NaH, THF, [18]crown-6 cat., reflux, 7 h (68 %); f) **25** (2.2 equiv), NaH, THF, 20 °C, 16 h (84 %).

 © 2007 Wiley-VCH Verlag GmbH & Co. KGaA, Weinheim

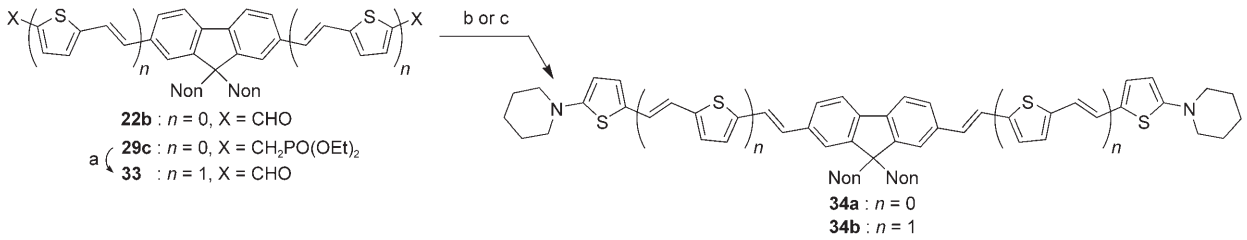

Scheme 8. a) **5b** (2.3 equiv), NaH, THF, 20 °C, 15 h, then 60 °C, 2 h; HCl, 20 °C, 2 h (55 %); b) **22b**, {[5-(1-piperidinyl)-2-thienyl]methyl}triphenylphosphonium iodide (2.3 equiv), *t*BuOK, CH_2Cl_2, 20 °C, 48 h, then I_2 cat., *hν* (22 % of **34a**); c) **33**, conditions as in (b) (18 % of **34b**).

Moreover, the latter are unnecessary if nonyl chains are present on the core, as exemplified with methylsulfonyl derivatives **26a**,**b**, the solubility of which is quite similar to that of the other dinonylfluorene derivatives.

Absorption and photoluminescence properties: The photophysical properties (absorption and fluorescence) of the new series of fluorophores are collected in Table 1 and include fluorescence quantum yields and lifetimes. Corresponding figures are given as Supporting Information. We observe that all fluorophores display an intense absorption in the near UV-visible blue region, with typical molar extinction coefficients ranging from 60,000–180,000 $mol^{-1}\,L\,cm^{-1}$. Their absorption and emission range can be tuned by playing on the nature of the end-groups, of the core moiety, and on the nature and length of the conjugated rods. In addition, all molecules exhibit good fluorescence quantum yields, ranging between 0.45 and 0.98.

Core effect: Substitution of the biphenyl core by a fluorene core produces a systematic red-shift of the absorption band while maintaining quasiidentical fluorescence properties (Supporting Information, Figure S1). Thus, the resulting Stokes shift is consistently reduced. Moreover, except for compounds **14** and **20**, the halfbandwidth of fluorenyl derivatives is systematically smaller than that of its biphenyl analogue. In fact, these distinctive features are directly related to geometrical properties: although the fluorene core is already planar in the ground state, the biphenyl unit has some torsional flexibility, the lowest-energy conformation corresponding to a twist angle of about 35°.[73] This leads to both blue-shift and broadening of the absorption band of biphenyl derivatives in contrast to fluorene analogues. The similari-

Table 1. Photophysical properties of quadrupolar compounds in toluene.

Compound				Length [nm]	λ_{max}^{abs} [nm]	$\log\varepsilon_{max}$	FWHM [cm^{-1}]	λ_{max}^{em} [nm]	Stokes shift [cm^{-1}]	$\Phi^{[a]}$	$\tau^{[b]}$ [ns]
Name	End-group	Linker	Core								
13a	$NHex_2$	PE	BP	2.4	374	4.92	3800	424	3200	0.90	0.70
16a	$NHex_2$	PV	BP	2.3	401	4.92	3900	456	3000	0.84	0.82
13b	$NHex_2$	PE_2	BP	3.8	381	5.03	4250	433	3200	0.82	0.73
14	$NOct_2$	PV–PE	BP	3.7	406	5.13	3600	463	3000	0.50	0.74
16b	$NHex_2$	PE–PV	BP	3.7	400	5.22	3950	452	2900	0.81	0.79
17a	$NOct_2$	PV–FV	BP	3.5	443	5.13	4400	522	3400	0.69	1.25
17b	$NHex_2$	PV–TV	BP	3.6	458	5.10	3900	522	2700	0.51	0.85
19a	$NHex_2$	PE	FL	2.4	387	4.92	3700	421	2100	0.80	0.74
23	OMe	PV	FL	2.3	381	4.82	3900	415	2200	0.90	0.87
28	NH_2	PV	FL	2.3	392	4.87	4000	433	2400	0.82	0.83
24	NBu_2	PV	FL	2.3	415	4.98	3600	457	2200	0.79	0.87
34a	Pip	TV	FL	2.2	387	4.78	3900	484	5200	0.45	1.00
19b	$NHex_2$	PE_2	FL	3.8	387	5.11	4100	433	2700	0.82	0.60
30	$NHex_2$	PV_2	FL	3.6	431	5.13	4000	480	2400	0.85	0.83
20	$NOct_2$	PV–PE	FL	3.7	411	5.10	4300	464	2800	0.61	0.80
32	NBu_2	PV–FlV	FL	4.5	429	5.26	3700	472	2100	0.78	0.73
31	$NOct_2$	PV–TV	FL	3.5	470	5.09	3800	525	2200	0.47	0.79
34b	Pip	TV_2	FL	3.5	451	4.98	3900	540	3600	0.45	0.67
21b	SO_2CF_3	PE	FL	2.4	372	4.84	3900	404	2200	0.98	0.79
21a	SO_2Oct	PE	FL	2.4	363	4.86	3500	389	1800	0.76	0.64
26a	SO_2Me	PV	FL	2.3	387	4.82	3600	423	2200	0.91	0.87
21c	SO_2Oct	PV–PE	FL	3.7	382	5.08	4500	419	2300	0.90	0.56
26b	SO_2Me	PV_2	FL	3.7	412	4.91	4000	456	2300	0.73	0.74

[a] Fluorescence quantum yield determined relative to fluorescein in 0.1 M NaOH. [b] Fluorescence lifetime determined by using time-correlated single-photon counting (TCSPC).

 © 2007 Wiley-VCH Verlag GmbH & Co. KGaA, Weinheim

ties of the emission properties clearly demonstrate that the biphenyl core becomes planar in the relaxed emitting excited state.

Connector effect: phenylene–vinylene versus phenylene–ethynylene: Changing the nature of the conjugated linker allows spectral tuning of both the absorption and emission characteristics. Replacing a triple bond by a double bond induces a bathochromic shift and hyperchromic effect of both the absorption and emission bands, in agreement with an extended electronic conjugation in the ground and excited states (Supporting Information, Figure S2). Interestingly, the fluorescence lifetime always increases, most likely due to the higher stretching frequency of a C≡C bond relative to that of a C=C bond, which is responsible for more efficient nonradiative decay.

On the other hand, replacement of a triple bond by a double bond in elongated derivatives (PE_2) produces very different effects on the fluorescence quantum yield, depending on its location in the conjugated rods. For instance, the shorter derivatives (i.e., connectors = PE and PV) show similar fluorescence quantum yields. For the longer derivatives, the replacement of a triple bond by a double bond does not significantly affect the fluorescence quantum yield if the substituted triple bond is positioned next to the central block (i.e., connector = PE–PV instead of PE_2). However, a decrease of 25–40% in the fluorescence quantum yield is obtained if the double bond is located close to the end-groups (i.e., linker PV–PE instead of PE_2).[103] This demonstrates that subtle changes in the topology of the conjugated rods may strongly influence the photoluminescence efficiency of the series of quadrupolar fluorophores investigated in the present work. Interestingly, further replacement of a triple bond by a double bond (i.e., connector = PV_2) restores high fluorescence quantum yields.

Connector effect: influence of arylene moieties: Replacing a phenyl unit by a thienyl unit in the conjugated connectors always induces a significant bathochromic shift of the emission band, but leads either to a blue-shift (PV versus TV and PV–TV versus TV2) or a red-shift (PV2 versus PV–TV or TV2) of the absorption band (Supporting Information, Figure S3), indicating that the reduction in the aromaticity in the connectors does not necessarily lead to a reduction of the electronic gap between the ground and excited states. On the other hand, the introduction of the low-aromaticity thiophene heterocycle in the conjugated systems always results in lower fluorescence quantum yields. In most cases, larger Stokes shifts are observed, but no major nor regular effects are visible on the fluorescence lifetime. This can be related to the combination of slower radiative decays, related to the red-shifted emission, and greater nonradiative decay due to enlarged intersystem crossing.[104]

Length effect: Increasing the connector length induces a systematic, but more or less pronounced, red-shift and hyperchromic effect on the absorption bands. On the other hand, other photoluminescence characteristics are differently affected, depending on the nature of the connector. If the length is increased by doubling the same connector (Supporting Information, Figure S4, Table 1), absorption bands undergo a broadening and emission bands are red-shifted. Because the hyperchromic effect tends to increase the radiative decay, whereas the emission red-shift has an opposite effect, the fluorescence quantum yields increase (compound **30** versus **24**) if the former effect dominates, whereas the opposite is observed if the latter dominates (compound **26b** versus **26a**). In the case of thienylene–vinylene oligomers, increasing the number of thienylene–vinylene units leads to the largest red-shifts of both the absorption and emission bands, as well as to a hyperchromic effect of the absorption band (Supporting Information, Figure S4b). The fluorescence quantum yield is maintained, but its lifetime decreases by about 30% due to the combination of faster radiative (in relation with the hyperchromic effect) and nonradiative constants. In comparison, the lengthening of the conjugated rods based on phenylene–ethynylene oligomers leads to a definite hyperchromic effect, but to only a slight bathochromic shift of the absorption bands (Supporting Information, Figure S4c). Similarly to phenylene–vinylene oligomers, a red-shift of the emission bands is observed, whereas the fluorescence quantum yields are maintained or decrease only slightly.

Insertion of thienylene–vinylene, furylene–vinylene, or fluorenylene–vinylene leads to bathochromic shifts of both the absorption and emission bands (Supporting Information, Figure S5). We note that the fluorenylene–vinylene leads to the smallest red-shift and highest fluorescence quantum yield, whereas the thienylene–vinylene unit leads to the largest red-shift and lowest quantum yield, most probably because of increased nonradiative decay due to enlarged intersystem crossing. Interestingly, the furylene–vinylene unit leads to a significantly longer fluorescence lifetime, most probably because of a reduction in the radiative decay due to the marked red-shift of the absorption band, which is not compensated by a hyperchromic effect of the absorption band, as well as to higher Stokes shifts relative to other conjugating units.

End-groups effect: Finally, we note that increasing either the electron-withdrawing (Supporting Information, Figure S6a) or electron-releasing (Supporting Information, Figure S6b) character of the peripheral groups leads to a bathochromic shift of both the absorption and emission bands, indicative of a more pronounced either core-to-periphery or periphery-to-core intramolecular charge transfer. This indicates that the core can act as either an acceptor[105] or a donor moiety,[106] depending on the peripheral counterparts. This was confirmed by molecular orbital calculations.

We observe that pull–pull compounds appear blue-shifted, compared to push–push derivatives. Interestingly, increasing the donor strength leads to a slight decrease in the fluorescence quantum yield, whereas increasing the acceptor strength leads to an increase.

 © 2007 Wiley-VCH Verlag GmbH & Co. KGaA, Weinheim

Two-photon absorption

The TPA spectra of the fluorophores were determined in the NIR range (700–1000 nm) by investigating their two-photon-excited fluorescence (TPEF) in 10^{-4} M toluene solutions. The measurements were performed under excitation with 150 fs pulses from a Ti:sapphire laser by using the experimental protocol of Xu and Webb.[107] The quadratic dependence of the TPEF signal on the excitation intensity was checked for each data point and confirmed that no photodegradation or saturation occurs. TPEF allows direct measurement of the TPEF-action cross section $\sigma_2\Phi$, the relevant figure of merit for imaging applications. From these values, the corresponding TPA cross sections σ_2 can be derived. This method has been recognized to be more reliable than nonlinear transmission measurements.[108] We emphasize that experiments were conducted in the femtosecond regime, thereby preventing contribution from linear nonresonant absorption or from excited-state absorption that is known to lead to artificially enhanced "effective" TPA cross sections if measurements are conducted in the nanosecond regime. We also stress that the reported values are *non-one-photon resonant* values, meaning that these chromophores could actually allow for the three-dimensional resolution offered by selective two-photon excitation in the NIR region. This is not the case if even slight one-photon absorption is present (such as for a number of chromophores with giant resonant TPA reported recently[109–112]).The TPA cross sections were determined by comparing their TPEF to that of fluorescein in water (pH 11),[107] according to the following Equation (1):

$$\sigma_s = \frac{S_s}{S_r}\frac{\eta_r}{\eta_s}\frac{\Phi_r}{\Phi_s}\frac{C_r}{C_s}\sigma_r \quad (1)$$

in which the subscripts s and r refer to the sample and reference molecules, respectively. The intensity of signal collected by a photomultiplier was denoted as S. The η and Φ are the overall fluorescence collection efficiency and the fluorescence quantum yield, respectively. The number density of the molecules in solution is denoted as C. The σ_r is the TPA cross-section value of the reference (i.e., fluorescein). The experimental data are collected in Table 2.

From Table 2, we observe that in most cases the lowest-energy TPA band is observed at a lower wavelength than twice that of the lowest-energy band in the one-photon-absorption spectrum. In fact, as these quadrupoles are nearly centrosymmetric, the one-photon excited state has only little TPA activity[41,89,90] and the two-photon-allowed excited state lies at higher energy. After two-photon excitation, relaxation to the lowest-energy excited state leads to the lowest-energy one-photon-allowed excited state, thus allowing for radiative deactivation to take place. Note that given the spectral window investigated here, the TPA maxima cor-

Table 2. Structure–TPA properties of quadrupolar compounds in toluene.

Compound				E_{gap}[a] [eV]	$2\lambda_{max}^{OPA}$ [nm]	λ_{max1}^{TPA} [nm]	λ_{max2}^{TPA} [nm]	σ_2 [GM][b]			N_e[c]	σ_2/N_e[d] [GM]
Name	End-group	Linker	Core					at 705 nm	at λ_{max1}^{TPA}	at λ_{max2}^{TPA}		
13a	$NHex_2$	PE	BP	3.12	748	–	–	890	–	–	28	31.8
16a	$NHex_2$	PV	BP	2.90	802	730	–	740	1040	–	28	37.1
13b	$NHex_2$	PE_2	BP	3.06	762	750	–	610	820	–	44	18.6
14	$NOct_2$	PV–PE	BP	2.87	812	815	–	1140	910	–	44	25.9
16b	$NHex_2$	PE–PV	BP	2.92	800	740	–	1230	1050	–	44	28.0
17a	$NOct_2$	PV–FV	BP	2.59	886	850	–	810	420	–	44	18.4
17b	$NHex_2$	PV–TV	BP	2.54	916	880	960	3040	1350	1020	44	69.1
19a	$NHex_2$	PE	Fl	3.07	774	–	–	1200	–	–	28	42.9
23	OMe	PV	Fl	3.12	762	–	–	110	–	–	28	3.9
28	NH_2	PV	Fl	3.01	784	–	–	400	–	–	28	14.3
24	NBu_2	PV	Fl	2.85	830	740	–	1130	1260	–	28	45.0
34a	Pip	TV	Fl	2.88	774	–	–	95	–	–	28	3.4
19b	$NHex_2$	PE_2	Fl	3.03	774	735	–	1080	1020	–	44	24.5
30	$NHex_2$	PV_2	Fl	2.73	862	730	815	2110	1920	1210	44	48.0
20	$NOct_2$	PV–PE	Fl	2.84	822	815	–	1970	1150	–	44	44.8
32	NBu_2	PV–FlV	Fl	2.76	858	730	–	3470	2960	–	56	62.0
31	$NOct_2$	PV–TV	Fl	2.50	940	880	–	5480	1530	–	44	124.5
34b	Pip	TV_2	Fl	2.53	902	735	–	850	680	–	44	19.3
21b	SO_2CF_3	PE	Fl	3.20	744	730	–	83	68	–	32	2.6
21a	SO_2Oct	PE	Fl	3.30	726	730	–	52	33	–	32	1.6
26a	SO_2Me	PV	Fl	3.07	774	–	–	220	–	–	32	6.9
21c	SO_2Oct	PV–PE	Fl	3.10	764	–	–	610	–	–	48	12.7
26b	SO_2Me	PV_2	Fl	2.87	824	725	815	1040	960	420	48	21.7

[a] The electronic gap (E_{gap}) is calculated from the absorption and emission maxima. [b] $1\ GM = 10^{-50}\ cm^4\,s\,photon^{-1}$; TPEF measurements were performed by using a mode-locked Ti:sapphire laser delivering 80 fs pulses at 80 MHz, calibrating with fluorescein.[107] [c] Effective number of π electrons in the conjugated system.[114] [d] Largest TPA cross section measured in the 700–1000 nm range, normalized by the effective number N_e of π electrons in the conjugated system.

© 2007 Wiley-VCH Verlag GmbH & Co. KGaA, Weinheim

responding to this higher-lying state is not systematically reached for all chromophores (Table 2).

End-groups effect: As noted from Table 2 and illustrated in Figure 2, push–push chromophores show larger TPA cross

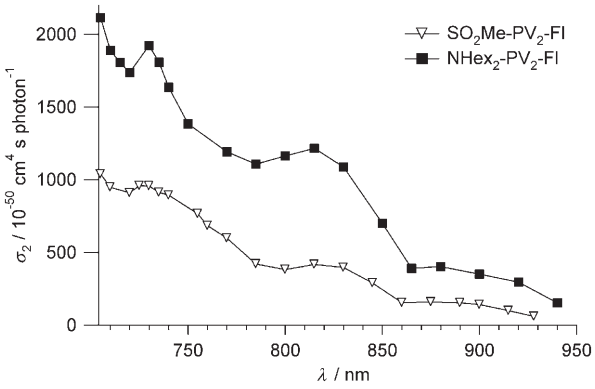

Figure 2. TPA spectra of **26b** and **30** in toluene: end-group (push–push vs. pull–pull) effect.

sections in the NIR region than corresponding pull–pull derivatives, following the definite red-shift of both the one-photon- and two-photon-absorption spectra and the reduction of the electronic gap between ground and excited states. Increasing the strength of electron-donating end-groups results in a pronounced enhancement of the TPA cross sections in the NIR region, again following the red-shift of both one- and two-photon-absorption spectra of push–push derivatives, as illustrated in Figure 3 and observed from Table 2. A similar effect is observed with electron-withdrawing groups (Figure 4).

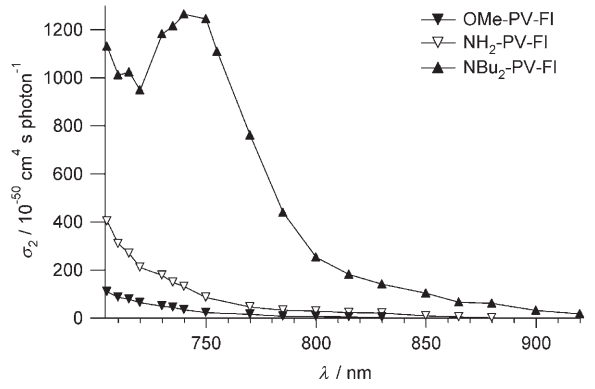

Figure 3. TPA spectra of **23**, **28**, and **24** in toluene: donor-strength effect.

Core effect: Comparison of push–push derivatives built from the different core moieties and bearing similar end-groups demonstrates that the nature of the conjugated core significantly influences the TPA spectra and governs the TPA cross-section magnitude. Independently of the connector nature, rigidification of the biphenyl unit, as obtained with

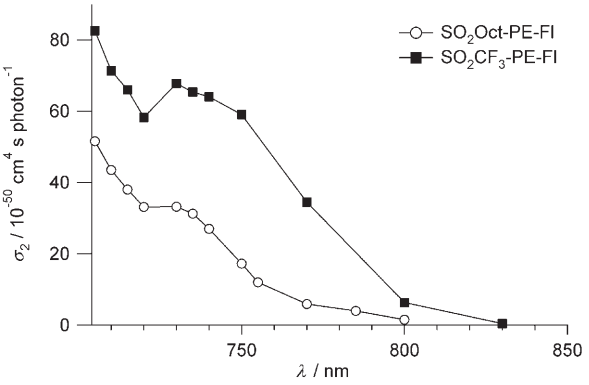

Figure 4. TPA spectra of **21a** and **21b** in toluene: acceptor-strength effect.

fluorene, always leads to a significant increase in the TPA cross section (Table 2). For instance, as observed from Figure 5, the push–push fluorene-core derivative **24** shows larger TPA cross sections than its biphenyl analogue **16a** in the whole red-NIR region.

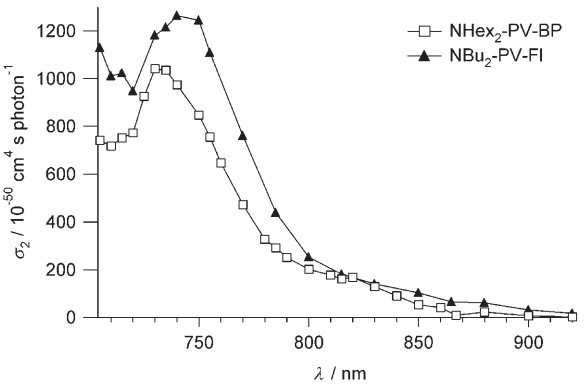

Figure 5. TPA spectra of **16a** and **24** in toluene: core effect.

Connector effect: phenylene–vinylene versus phenylene–ethynylene: We observe from Table 2 that replacement of a triple bond by a double bond always leads to a significant increase in the TPA cross sections in the NIR region, whatever the nature of the end-groups (D or A) of the core moiety and of the length of the conjugated rods. In addition, the replacement of triple bonds by double bonds also induces a significant broadening and red-shift of the TPA spectra, as illustrated in Figure 6. This effect parallels the red-shift of both absorption and emission bands, that is, it correlates with the reduction of the electronic gap between ground and excited states. As a result, all fluorophores built from vinylene linkers instead of ethynylene linkers show much larger TPA cross sections in the whole red-NIR region, the effect being more pronounced for higher wavelengths, as clearly seen from Figure 6. This is of particular importance for imaging applications because 1) improved penetration depth is achieved upon shifting to higher wavelength (due to reduction of scattering losses) and 2) spectral

 © 2007 Wiley-VCH Verlag GmbH & Co. KGaA, Weinheim

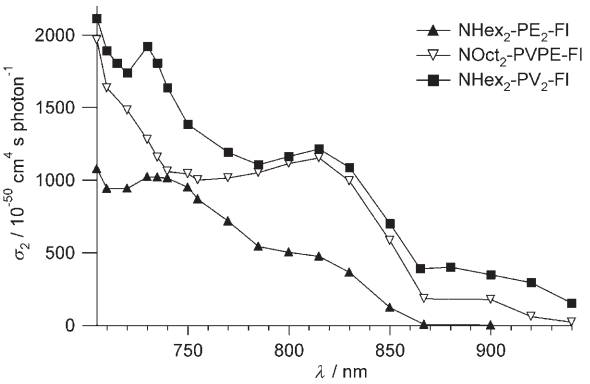

Figure 6. TPA spectra in toluene of **19b**, **20**, and **30**: linker effect.

broadening offers much more flexibility in terms of two-photon excitation (allowing for a wider choice of laser sources).

Connector effect: influence of arylene moieties: The nature of the arylene unit in the conjugated rods also plays an important role in tuning the TPA spectra and influencing the TPA cross-section magnitude. For derivatives of comparable length and bearing similar peripheral groups, we observe that replacement of the phenyl unit by a thienyl unit in the conjugated backbone has a markedly different impact, depending on its position in the conjugated backbone. In particular, if a *terminal* phenyl ring is substituted by a thienyl ring, a major *decrease* in the TPA efficiency is obtained (Table 2). For instance, compound **34a** displays TPA cross sections of about one order of magnitude lower than compound **24** (Figure 7a) throughout the red-NIR range. A similar effect is observed if compounds **34b** and **31** are compared (Figure 7b). In contrast, if the phenyl ring is replaced by a thienyl ring close to the core, a distinct increase in the TPA magnitude, as well as a red-shift and *definite broadening of the TPA spectrum in the NIR region*, is observed (Table 2). For instance, compound **31** displays a TPA cross section that is more than twice that of compound **30** at 705 nm and more than three times that at 900 nm. As a result, fluorophore **31** maintains a large *TPEF-action cross section* ($\sigma_2\Phi$) at 1 μm (i.e., 265 GM), a region of particular interest for imaging applications due to the increased penetration depth in tissues and availability of lower-cost lasers. This effect parallels the bathochromic shift of both the absorption and emission bands, that is, the significant reduction in the electronic gap.

We emphasize that the present study demonstrates that *the topology of the conjugated connectors dramatically influences the TPA properties*. Indeed, replacing the phenyl ring by the less aromatic thienyl ring may have either a positive or negative effect on TPA properties, depending on its location in the conjugated system. Furthermore, *decreasing the aromaticity of the connector does not necessarily lead to enhanced TPA properties*, even if the aromatic connector is located close to the core. This is clearly shown from comparison of compounds **17a** and **17b**: replacing the thienyl ring

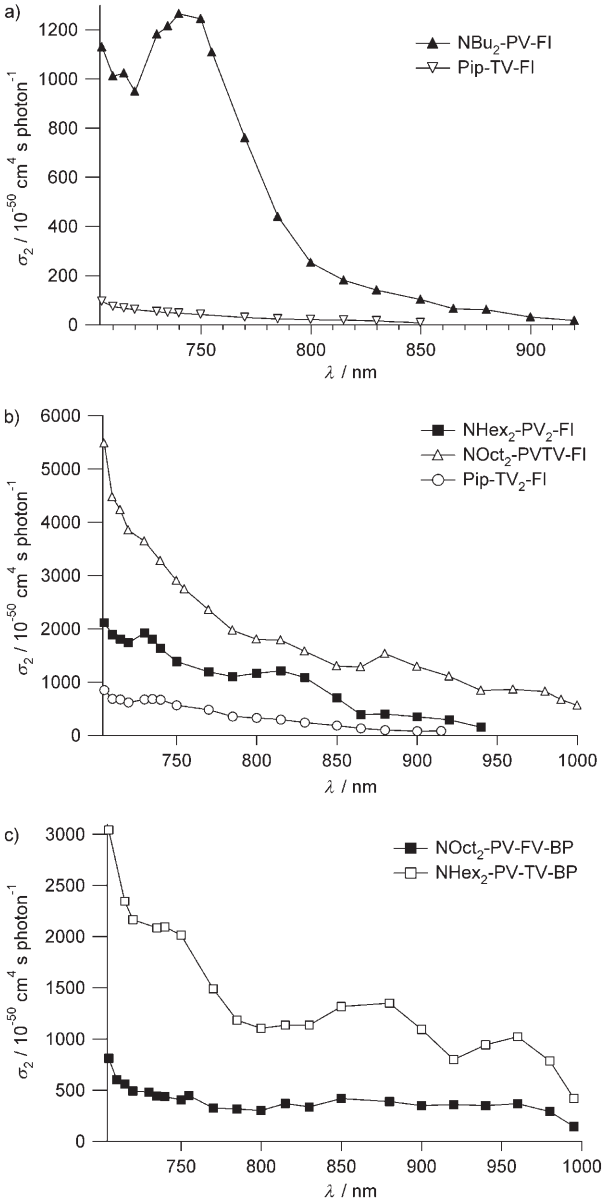

Figure 7. TPA spectra in toluene of a) **24** and **34a**; b) **30**, **31**, and **34b**; c) **17a** and **17b**: connector effects.

by a furyl ring, whose aromaticity is much lower,[113] in the conjugated system results in a major *decrease* in the TPA cross sections within the whole red-NIR spectral range (Figure 7c). This clearly demonstrates the limitations of the popular strategy consisting of reducing the aromaticity of conjugated systems for improvement of nonlinear, and particularly TPA, properties. Clearly, a more subtle approach is needed for molecular optimization of TPA properties.

Topology effect: The importance of the topology of the conjugated system is also seen clearly from comparison of compounds **14** and **16b** that have the same end-groups, core, and analogous connectors, except for the location of the triple-bond linker either close to the core (molecule **14**) or close to the end-groups (molecule **16b**). Although com-

 © 2007 Wiley-VCH Verlag GmbH & Co. KGaA, Weinheim

pounds **14** and **16b** have similar one-photon characteristics (Table 1), they clearly show *different* TPA spectra within the NIR range (Figure 8). Indeed, if the triple bond linker is located closer to the core, the low-energy TPA band is red-

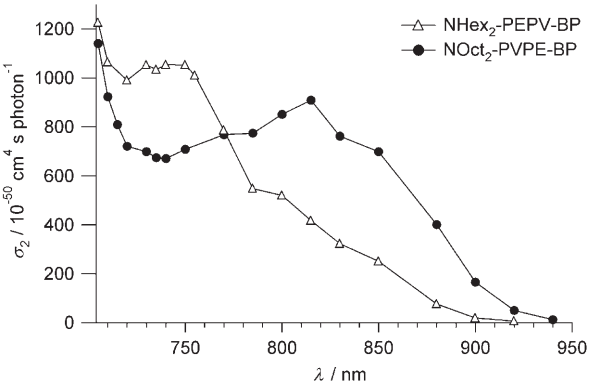

Figure 8. TPA spectra of **16b** and **14** in toluene: topology effect.

shifted, its maximum being shifted by 75 nm. Consequently, compound **14** shows higher TPA efficiency at wavelengths longer than 770 nm. As an illustration, the TPA cross section of molecule **14** is more than twice that of its analogue **16b** at 850 nm. Hence, compound **14**, although showing *similar* linear transparency to compound **16b**, has broader TPA in the NIR. Such an effect is of particular interest in optical-limiting applications for which improved nonlinearity/transparency trade-off is an important issue. In this respect, it is also interesting to note that chromophore **14** has a lower fluorescence quantum yield while maintaining a similar excited-state lifetime, thus offering better characteristics for broadband optical limiting in the visible-NIR region based on multiphoton absorption (including two-photon-induced excited-state absorption in the nanosecond regime).[35] This shows that subtle changes in the structures of the conjugated arms may have important implications in terms of molecular engineering for specific applications.

Length effect: The lengthening of the conjugated rods based on either phenylene–vinylene (Figure 9a) and thienylene–vinylene (Figure 9b) oligomers leads to a major increase in the TPA magnitude throughout the whole red-NIR range, which parallels the lowering of the electronic gap between the ground and the first excited states (Table 2). It should be stressed that the TPA magnitude increases by more than the size of the molecule in the case of oligomeric phenylene–vinylene or thienylene–vinylene connectors, as indicated by σ_2/N_e, the peak TPA cross section normalized by the effective number of electrons[114] (Table 2). In addition, we observe a marked red-shift of the TPA bands that results in a significant improvement in the TPA properties at higher wavelength. As a result, elongated fluorophores show not only higher TPA peaks, but also much broader TPA activity in the target spectral range. This superlinear increase indicates that the lengthening approach is a valid strategy for TPA enhancement in the red-NIR range.

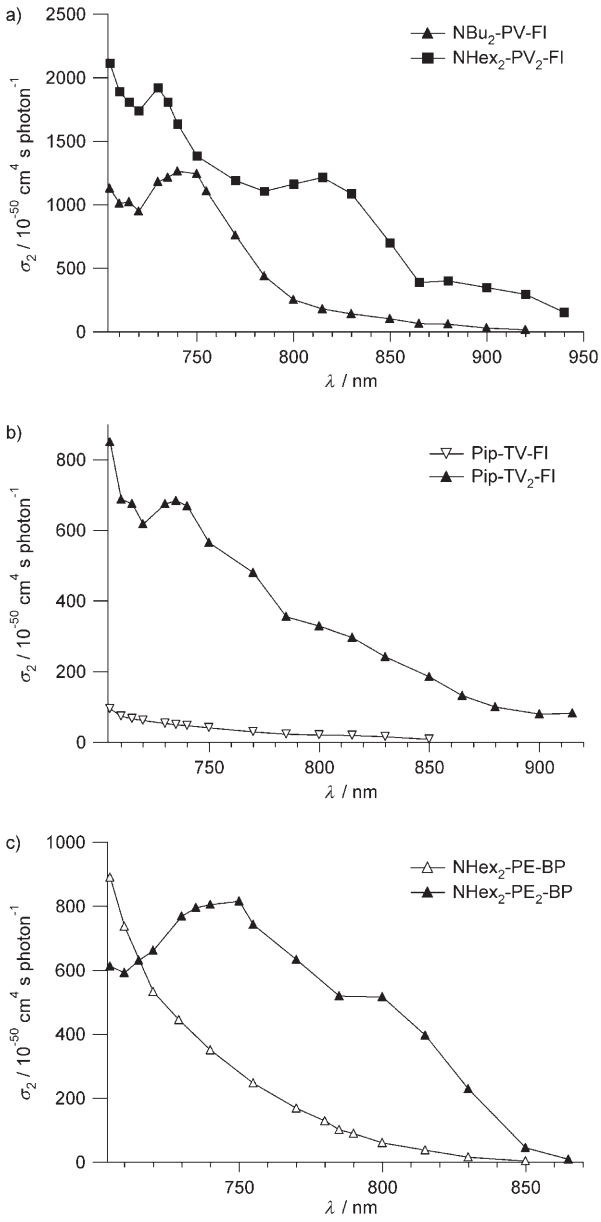

Figure 9. TPA spectra in toluene of a) **24** and **30**; b) **34a** and **34b**; and c) **13a** and **13b**: length effects.

However, it should be stressed that the amplitude of the increase depends markedly on the nature of the extensor. For instance, the lengthening of the conjugated rods based on phenylene–ethynylene oligomers does not necessarily lead to an increase in the TPA response (Table 2 and Figure 9c): a marked red-shift and broadening of the TPA response is obtained in the red-NIR range (Figure 9c), whereas the one-photon-absorption band is only slightly red-shifted (Supporting Information, Figure S4c). Consequently, a major increase in TPA efficiency in the NIR region is observed (by a factor of three to more than ten in the 750–850 nm region) with nearly no loss of linear transparency.

 © 2007 Wiley-VCH Verlag GmbH & Co. KGaA, Weinheim

Hence, phenylene–ethynylene oligomers appear as suitable connectors for broadband optical limiting in the visible-NIR region.

Finally, incorporation of a fluorenylene–vinylene or a thienylene–vinylene extensor in the conjugated arms also leads to a major increase in the TPA efficiency throughout the whole red-NIR range, that is, the spectral range of interest (Figure 10). Interestingly, the strongest effect (both net

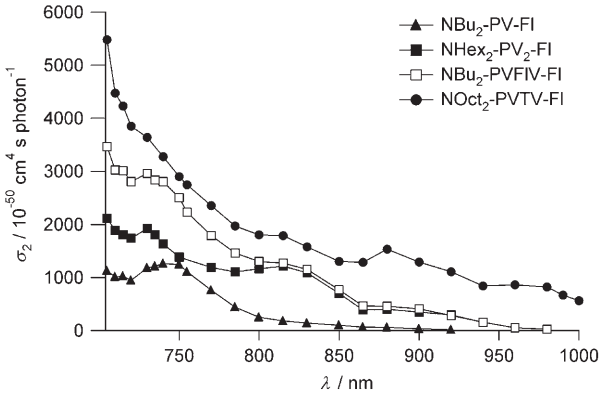

Figure 10. TPA spectra of **24**, **30**, **32**, and **31** in toluene.

increase and spectral broadening further to the NIR region) is obtained for the thienylene–vinylene connector, in correlation with the smallest energy gap between relaxed ground and excited states. Compared to insertion of a phenylene–vinylene, the insertion of a fluorenylene–vinylene allows for a major TPA increase, mainly to the blue of the lowest-energy TPA peak. In contrast, insertion of a thienylene–vinylene unit allows a larger TPA increase throughout the whole red-NIR range than insertion of a phenylene–vinylene unit (Figure 10). In comparison to both thienylene–vinylene oligomers and phenylene–vinylene oligomers, extended arms based upon the *alternation* of thienylene–vinylene and phenylene–vinylene moieties lead to major TPA enhancement and broadening in the red-NIR range. Indeed, chromophore **31** shows a normalized TPA cross section (σ_2/N_e) measured in the femtosecond regime similar to that of the best (in terms of *non-one-photon resonant* TPA) chromophore reported so far,[115] although being blue-shifted by nearly 40 nm. Thus, this molecule is particularly promising for optical limiting in the 700–900 nm region in the nanosecond regime. The present study provides evidence that by playing not only on the length of the conjugated arms, but more importantly on their nature and their topology, major (and nonlinear) increases in the TPA efficiency throughout the whole NIR range can be achieved.

Conclusion

This systematic study of the absorption, photoluminescence, and two-photon-absorption properties on such a broad series of quadrupolar fluorophores allowed us to derive structure–property relationships of great significance for both spectral tuning and amplification of the molecular TPA in the NIR spectral range. The influence of each moiety constituting these quadrupolar structures (cores, linkers, connectors, and end-groups) was studied in detail. Push–push systems were found to be more efficient than pull–pull systems, and planarization of the core (fluorene vs. biphenyl) always leads to an increase in the TPA cross sections. The role of the conjugated rods should also be emphasized: their length is, of course, an important parameter, however, the nature of the linkers (double or triple bonds) and of the arylene units (phenylene, thienylene, furylene, fluorenylene) is also of particular importance. Concerning this last point, we have shown that the classical strategy consisting of reducing the aromaticity of the connectors does not necessarily give rise to an enhancement of the TPA response within the spectral region of interest. Moreover, we have demonstrated that the topology of the conjugated system, that is, the location of linkers and connectors in the conjugated rods, can dramatically influence the TPA properties. Small changes in the structure may have important implications in terms of molecular engineering for specific applications, because the TPA properties (in terms of cross sections, position of the maximum, and bandwidth), as well as the one-photon and the photoluminescence characteristics can be affected considerably. Thus, it becomes possible to optimize the transparency/TPA efficiency and the fluorescence/TPA efficiency trade-offs. With these findings, quadrupolar fluorophores combining very large peak TPA cross sections (up to 5480 GM), broad TPA bands throughout the whole 700–1000 nm range, and high fluorescence quantum yields (ranging from 0.45 to 0.98) could, thus, be obtained. Such compounds are of particular interest for TPEF microscopy,[45] as well as optical limiting in the visible[39] and NIR[35] regions.

Experimental Section

Photophysical methods: UV/Vis spectra were recorded by using a Jasco V-570 spectrophotometer. Steady-state fluorescence measurements were performed at RT on dilute solutions (ca. 10^{-6} M) by using an Edinburgh Instruments (FLS 920) spectrometer working in photon-counting mode, equipped with a calibrated quantum counter for excitation correction. Fully corrected emission spectra were obtained, for each compound, at $\lambda_{ex}=\lambda_{max}^{abs}$ with $A_{\lambda_{ex}} \leq 0.1$ to minimize internal absorption. Fluorescence quantum yields were measured by using standard methods[116] on air-equilibrated samples at RT. Fluorescein in 0.1 M NaOH ($\Phi=0.90$ at $\lambda_{ex}=$ 470 nm) was used as a reference.[117] The reported fluorescence quantum yields are within $\pm 10\%$. Fluorescence lifetimes were measured by time-correlated single-photon counting (TCSPC) by using the same FLS 920 fluorimeter. Excitation was achieved by a hydrogen-filled nanosecond flashlamp (repetition rate 40 kHz). The instrument response (FWHM ca. 1 ns) was determined by measuring the light scattered by a Ludox suspension. The TCSPC traces were analyzed by standard iterative reconvolution methods implemented in the software of the fluorimeter. All compounds displayed strictly monoexponential fluorescence decays ($\chi^2 < 1.1$). Two-photon-absorption (TPA) measurements were conducted by investigating the two-photon-excited fluorescence (TPEF) of the fluorophores in toluene at RT on air-equilibrated solutions (10^{-4} M), by using a Ti:sapphire laser delivering 150-fs excitation pulses, according to the experimental protocol established by Xu and Webb.[107] This protocol avoids

 © 2007 Wiley-VCH Verlag GmbH & Co. KGaA, Weinheim

contributions from excited-state absorption that are known to result in largely overestimated TPA cross sections. The quadratic dependence of the fluorescence intensity on the excitation intensity was verified for each data point, indicating that the measurements were carried out in intensity regimes in which saturation or photodegradation do not occur. TPEF measurements were calibrated relative to the absolute TPEF-action cross sections determined by Xu and Webb for fluorescein (10^{-4} M in 0.01 M aqueous NaOH) in the 690–1000 nm range.[107,118] This procedure provides the TPEF-action cross section $\sigma_2\Phi$ from which the corresponding σ_2 value is derived. The experimental uncertainty of the absolute action cross sections determined by this method has been estimated to be ±20 %.[107]

Synthetic procedures

General methods: All air- or water-sensitive reactions were carried out under argon. Solvents were generally dried and distilled prior to use. Reactions were monitored by performing thin-layer chromatography on Merck silica gel or neutral aluminum oxide 60 F_{254} precoated aluminum sheets. Column chromatography: Merck silica gel Si 60 (40–63 μm, 230–400 mesh), except otherwise noted. Melting points were determined by using an Electrothermal IA9300 digital melting-point instrument. NMR: Bruker AM 200 (^{1}H: 200.13 MHz), AM250 (^{1}H: 250.13 MHz, ^{13}C: 62.90 MHz, ^{31}P: 101.25 MHz), ARX 200 (^{1}H: 200.13 MHz, ^{13}C: 50.32 MHz), or Avance AV 300 (^{1}H: 300.13 MHz, ^{13}C: 75.48 MHz, ^{19}F: 282.38 MHz, ^{31}P: 121.50 MHz), in $CDCl_3$ solutions; ^{1}H chemical shifts (δ) are given in ppm relative to TMS as internal standard, ^{13}C chemical shifts are given relative to the central peak of $CDCl_3$ at 77.0 ppm, ^{31}P relative to H_3PO_4 as external standard, and ^{19}F relative to $CFCl_3$ as internal standard. High- and low-resolution mass spectra measurements were performed at the Centre Régional de Mesures Physiques de l'Ouest (C.R.M.P.O., Rennes) by using a Micromass MS/MS ZABSpec TOF instrument with EBE TOF geometry; liquid secondary ion mass spectrometry (LSIMS) at 8 kV with Cs^+ in *m*-nitrobenzyl alcohol (*m*NBA) or *o*-nitrophenyloctyl ether (*o*NPOE); ES^+ (electrospray ionization, positive mode) at 4 kV; EI (electron ionization) at 70 eV; CI (chemical ionization) with NH_3 or CH_4 as ionization gas. Elemental analyses were performed at I.C.S.N.–C.N.R.S. (Gif-sur-Yvette, France) or at the C.R.M.P.O. Compounds **1b**,[92] **1e**,[93] **3a–c**,[94] **5a**,[95] **5b**,[96] **7a**,[97] **9a**,[98] **12**,[100] and **15a**[101] were synthesized according to the respective literature procedures. [(4-Methoxyphenyl)methyl]triphenylphosphonium bromide was prepared according to ref. [119]. {[5-(1-Piperidinyl)-2-thienyl]-methyl}triphenylphosphonium iodide was prepared analogously to ref. [94]. Phosphonates **9b** and **11** were prepared analogously to ref. [98] and ref. [120], respectively. 9,9-Dinonyl-9*H*-fluorene (**18a**) was prepared by reaction of fluorene with 1-bromononane using *n*-butyllithium in THF, analogously to ref. [121]. Synthetic procedures and characterization data for all quadrupolar chromophores are given hereafter, and those for intermediate compounds can be found in the Supporting Information.

4,4′-[(1,1′-Biphenyl)-4,4′-diyldi-2,1-ethynediyl]bis(*N*,*N*-dihexylbenzenamine) (13a): Air was removed from a solution of **12**[100] (90 mg, 0.445 mmol) and **1b**[92] (431 mg, 1.112 mmol) in 4 mL of toluene/Et_3N (5:1) by blowing argon for 20 min. Then CuI (3.4 mg, 0.018 mmol) and $[Pd(PPh_3)_2Cl_2]$ (12.5 mg, 0.018 mmol) were added, and deaeration was continued for 10 min. Thereafter, the mixture was stirred at 20 °C for 2 h. The solvent was removed under reduced pressure, and the crude product was purified by column chromatography (heptane/CH_2Cl_2 90:10 then 80:20) to yield 270.4 mg (84 %) of **13a**: M.p. 113.5–114.5 °C; ^{1}H NMR (200.13 MHz, $CDCl_3$): δ = 7.56 (s, 8H), 7.38 and 6.58 (AA′XX′, J_{AX} = 9.0 Hz, 8H), 3.28 (m, 8H), 1.66–1.52 (m, 8H), 1.32 (m, 24H), 0.91 ppm (t, J = 6.5 Hz, 12H); ^{13}C NMR (50.32 MHz, $CDCl_3$): δ = 147.9, 139.2, 132.9, 131.6, 126.6, 123.4, 111.2, 108.6, 91.9, 87.0, 50.9, 31.7, 27.2, 26.8, 22.7, 14.0 ppm; HRMS (LSIMS$^+$, *m*NBA): *m*/*z*: calcd for $C_{52}H_{68}N_2$ [M^+]: 720.5383; found: 720.5390; elemental analysis calcd (%) for $C_{52}H_{68}N_2$ (721.12): C 86.61, H 9.50, N 3.88; found: C 86.42, H 9.64, N 3.90.

4,4′-[(1,1′-Biphenyl)-4,4′-diylbis(2,1-ethynediyl-4,1-phenylene-2,1-ethynediyl)]bis(*N*,*N*-dihexylbenzenamine) (13b): Reaction of **12** (26.1 mg, 0.129 mmol) with **2a** (146 mg, 0.299 mmol), as described for **13a**, with subsequent purification by column chromatography (heptane/CH_2Cl_2, gradient from 50:50 to 0:100) and crystallization, afforded 102.6 mg (86 %) of **13b**: M.p. 234–235 °C; ^{1}H NMR (300.13 MHz, $CDCl_3$): δ = 7.61 (s, 8H), 7.49 and 7.46 (AA′XX′, J_{AX} = 8.7 Hz, 8H), 7.36 and 6.56 (AA′XX′, J_{AX} = 9.3 Hz, 8H), 3.27 (m, 8H), 1.66–1.52 (m, 8H), 1.31 (m, 24H), 0.90 ppm (t, J = 6.6 Hz, 12H); ^{13}C NMR (50.32 MHz, $CDCl_3$): δ = 148.1, 140.0, 132.9, 132.1, 131.4, 131.1, 126.9, 124.3, 122.5, 121.8, 111.1, 108.3, 93.2, 90.6, 90.4, 87.0, 50.9, 31.7, 27.2, 26.8, 22.7, 14.0 ppm; MS (ES^+, CH_2Cl_2/MeOH): *m*/*z*: 921.6 [M+H]$^+$, 461.4 [M+2H]$^{2+}$; HRMS (ES^+, CH_2Cl_2/MeOH): *m*/*z*: calcd for $C_{68}H_{77}N_2$ [M+H]$^+$: 921.6087; found: 921.6110; elemental analysis calcd (%) for $C_{68}H_{76}N_2$ (921.36): C 88.65, H 8.31, N 3.04; found: C 88.72, H 8.41, N 2.80.

4,4′-[(1,1′-Biphenyl)-4,4′-diylbis[2,1-ethynediyl-4,1-phenylene-(1*E*)-2,1-ethenediyl]]bis(*N*,*N*-dioctylbenzenamine) (14): Reaction of **12** (34.6 mg, 0.171 mmol) with **4a** (215 mg, 0.394 mmol), as described for **13a**, for 3.5 h, with subsequent purification by column chromatography (heptane/CH_2Cl_2, gradient from 40:60 to 0:100) and crystallization, afforded 144.4 mg (81 %) of **14**: M.p. 221–222 °C; ^{1}H NMR (200.13 MHz, $CDCl_3$): δ = 7.61 (s, 8H), 7.51 and 7.44 (AA′XX′, J_{AX} = 8.8 Hz, 8H), 7.38 and 6.62 (AA′XX′, J_{AX} = 8.8 Hz, 8H), 7.08 (d, J = 16.3 Hz, 2H), 6.86 (d, J = 16.3 Hz, 2H) 3.28 (m, 8H), 1.67–1.52 (m, 8H), 1.31 (m, 40H), 0.89 ppm (t, J = 6.3 Hz, 12H); ^{13}C NMR (50.32 MHz, $CDCl_3$): δ = 148.0, 139.8, 138.5, 132.0, 131.8, 129.9, 128.8, 127.9, 126.8, 125.8, 124.1, 122.7, 120.8, 111.6, 90.9, 89.7, 51.1, 31.8, 29.5, 29.3, 27.3, 27.2, 22.6, 14.1 ppm; HRMS (LSIMS$^+$, *m*NBA): *m*/*z*: calcd for $C_{76}H_{96}N_2$ [M^+]: 1036.7574; found: 1036.7565; elemental analysis calcd (%) for $C_{76}H_{96}N_2$ (1037.61): C 87.97, H 9.33, N 2.70; found: C 87.95, H 9.56, N 2.71.

4,4′-[(1,1′-Biphenyl)-4,4′-diyldi-(1*E*)-2,1-ethenediyl]bis(*N*,*N*-dihexylbenzenamine) (16a): NaH (0.45 g, 60 % dispersion in mineral oil) was added to a solution of **15b** (1.70 g, 3.74 mmol) and **1e**[93] (2.494 g, 7.48 mmol) in anhyd THF (70 mL). The mixture was stirred at 20 °C for 20 h, then under reflux for 4 h. After addition of water (25 mL), the THF was evaporated. The resulting precipitate was filtered and washed successively with EtOH and pentane. The crude product was then purified by column chromatography (heptane/CH_2Cl_2 60:40) to yield 1.90 g (70 %) of **16a**: M.p. 147–148 °C; ^{1}H NMR (200.13 MHz, $CDCl_3$): δ = 7.59 and 7.53 (AA′XX′, J_{AX} = 8.6 Hz, 8H), 7.39 and 6.62 (AA′XX′, J_{AX} = 8.8 Hz, 8H), 7.08 (d, J = 16.2 Hz, 2H), 6.90 (d, J = 16.2 Hz, 2H), 3.28 (m, 8H), 1.59 (m, 8H), 1.32 (m, 24H), 0.91 ppm (t, J = 6.4 Hz, 12H); ^{13}C NMR (50.32 MHz, $CDCl_3$): δ = 147.8, 138.7, 137.2, 128.8, 127.8, 126.8, 126.3, 124.4, 123.1, 111.6, 51.0, 31.7, 27.3, 26.8, 22.7, 14.1 ppm; HRMS (LSIMS$^+$, *m*NBA): *m*/*z*: calcd for $C_{52}H_{72}N_2$ [M^+]: 724.5696; found: 724.5694; elemental analysis calcd (%) for $C_{52}H_{72}N_2$ (725.15): C 86.13, H 10.01, N 3.86; found: C 85.81, H 10.03, N 3.78.

4,4′-[(1,1′-Biphenyl)-4,4′-diylbis[(1*E*)-2,1-ethenediyl-4,1-phenylene-2,1-ethynediyl]]bis(*N*,*N*-dihexylbenzenamine) (16b): NaH (26 mg, 60 % dispersion in mineral oil) was added to a solution of **15b** (75.4 mg, 0.166 mmol), **2b** (148.5 mg, 0.381 mmol), and [18]crown-6 (4.3 mg) in anhyd THF (8 mL). The mixture was stirred at 40 °C for 3 h. After addition of water, the precipitate was filtered and washed with water, EtOH, Et_2O, and pentane successively, and dried under vacuum. The product was then purified by column chromatography (heptane/CH_2Cl_2, gradient from 40:60 to 0:100) to yield 128 mg (84 %) of **16b**: M.p. 243–244 °C; ^{1}H NMR (200.13 MHz, $CDCl_3$): δ = 7.65 and 7.59 (AA′XX′, J_{AX} = 8.7 Hz, 8H), 7.49 (s, 8H), 7.37 and 6.57 (AA′XX′, J_{AX} = 9.1 Hz, 8H), 7.15 (s, 4H), 3.28 (m, 8H), 1.65–1.50 (m, 8H), 1.32 (m, 24H), 0.91 ppm (t, J = 6.6 Hz, 12H); MS (ES^+, $CHCl_3$/MeOH): *m*/*z*: 925.6 [M+H]$^+$, 463.4 [M+2H]$^{2+}$; HRMS (ES^+, $CHCl_3$/MeOH): *m*/*z*: calcd for $C_{68}H_{81}N_2$ [M+H]$^+$: 925.6400; found: 925.6391; elemental analysis calcd (%) for $C_{68}H_{80}N_2$ (925.39): C 88.26, H 8.71, N 3.03; found: C 88.03, H 8.95, N 2.97.

4,4′-[(1,1′-Biphenyl)-4,4′-diylbis[(1*E*)-2,1-ethenediyl-5,2-furanediyl-(1*E*)-2,1-ethenediyl]]bis(*N*,*N*-dioctylbenzenamine) (17a): NaH (150 mg, 60 % dispersion in mineral oil) was added to a solution of **15b** (216 mg, 0.475 mmol) and **6a** (422 mg, 0.965 mmol) in anhyd THF (10 mL). The mixture was stirred at 20 °C for 19 h. After addition of water, the precipitate was filtered and washed with water, EtOH, and pentane successively, and dried under vacuum, to yield 390 mg (80 %) of **17a**: M.p. 247–249 °C; ^{1}H NMR (200.13 MHz, $CDCl_3$): δ = 7.63 and 7.56 (AA′XX′, J_{AX} = 8.3 Hz, 8H), 7.37 and 6.62 (AA′XX′, J_{AX} = 8.6 Hz, 8H), 7.13 (d, J = 16.3 Hz, 2H),

 © 2007 Wiley-VCH Verlag GmbH & Co. KGaA, Weinheim

7.08 (d, $J=15.8$ Hz, 2H), 6.91 (d, $J=16.3$ Hz, 2H), 6.67 (d, $J=15.8$ Hz, 2H), 6.39 (d, $J=3.3$ Hz, 2H), 6.28 (d, $J=3.3$ Hz, 2H), 3.29 (m, 8H), 1.56 (m, 8H), 1.31 (m, 40H), 0.89 ppm (t, $J=6.6$ Hz, 12H); ^{13}C NMR (50.32 MHz, $CDCl_3$): $\delta=154.3$, 152.1, 147.8, 139.4, 136.4, 131.3, 129.4, 128.0, 127.7, 127.0, 126.7, 125.7, 124.1, 116.3, 111.6, 109.2, 51.0, 31.8, 29.5, 29.3, 27.3, 27.2, 22.7, 14.1 ppm; HRMS (LSIMS$^+$, *m*NBA): *m*/*z*: calcd for $C_{72}H_{96}N_2O_2$ [M^+]: 1020.7472; found: 1020.7477.

4,4′-[(1,1′-Biphenyl)-4,4′-diylbis[(1*E*)-2,1-ethenediyl-5,2-thiophenediyl-(1*E*)-2,1-ethenediyl]]bis(*N*,*N*-dihexylbenzenamine) (17b): Reaction of **15b** (227 mg, 0.5 mmol) with **6c** (415 mg, 1.04 mmol), as described for **17a**, for 16 h, afforded 301 mg (64%) of **17b**: M.p. 250–252 °C; ^{1}H NMR (200.13 MHz, $CDCl_3$): $\delta=7.62$ and 7.53 (AA′XX′, $J_{AX}=8.3$ Hz, 8H), 7.33 and 6.61 (AA′XX′, $J_{AX}=8.7$ Hz, 8H), 7.23 (d, $J=16.6$ Hz, 2H), 6.97 (d, $J=16.0$ Hz, 2H), 6.94 (d, $J=3.7$ Hz, 2H), 6.89 (d, $J=16.6$ Hz, 2H), 6.86 (d, $J=3.7$ Hz, 2H), 6.84 (d, $J=16.0$ Hz, 2H), 3.28 (m, 8H), 1.57 (m, 8H), 1.32 (m, 24H), 0.91 ppm (t, $J=6.2$ Hz, 12H); HRMS (LSIMS$^+$, *m*NBA): *m*/*z*: calcd for $C_{64}H_{80}N_2S_2$ [M^+]: 940.5763; found: 940.5758.

4,4′-[(9,9-Dinonyl-9*H*-fluorene-2,7-diyl)di-2,1-ethynediyl]bis(*N*,*N*-dihexylbenzenamine) (19a): Reaction of **18d** (231.6 mg, 0.496 mmol) with **1b**[92] (462.9 mg, 1.195 mmol), as described for **13a**, for 3 h, with subsequent purification by column chromatography (heptane/CH_2Cl_2 90:10), afforded 221 mg (45%) of **19a**; ^{1}H NMR (200.13 MHz, $CDCl_3$): $\delta=7.60$ (d, $J=8.3$ Hz, 2H), 7.46 (d, $J=8.3$ Hz, 2H), 7.45 (s, 2H), 7.39 and 6.57 (AA′XX′, $J_{AX}=9.0$ Hz, 8H), 3.27 (m, 8H), 1.96 (m, 4H), 1.58 (m, 8H), 1.32 (m, 24H), 1.30–0.99 (m, 24H), 0.90 (t, $J=6.6$ Hz, 12H), 0.83 (t, $J=6.7$ Hz, 6H), 0.61 ppm (m, 4H); ^{13}C NMR (50.32 MHz, $CDCl_3$): $\delta=150.9$, 147.8, 140.0, 132.8, 130.3, 125.5, 122.7, 119.6, 111.2, 108.7, 91.1, 88.2, 55.1, 50.9, 40.5, 31.8, 31.7, 30.1, 29.6, 29.3, 29.2, 27.2, 26.8, 23.7, 22.7, 22.6, 14.1, 14.0 ppm; HRMS (LSIMS$^+$, *m*NBA): *m*/*z*: calcd for $C_{71}H_{104}N_2$ [M^+]: 984.8200; found: 984.8209; elemental analysis calcd (%) for $C_{71}H_{104}N_2$ (985.62): C 86.52, H 10.64, N 2.84; found: C 86.12, H 10.85, N 2.88.

4,4′-[(9,9-Dinonyl-9*H*-fluorene-2,7-diyl)bis(2,1-ethynediyl-4,1-phenylene-2,1-ethynediyl)]bis(*N*,*N*-dihexylbenzenamine) (19b): Reaction of **18d** (100 mg, 0.214 mmol) with **2a** (241 mg, 0.494 mmol), as described for **13a**, for 20 h, with subsequent purification by column chromatography (heptane/CH_2Cl_2, gradient from 90:10 to 80:20), afforded 208.6 mg (82%) of **19b**; ^{1}H NMR (200.13 MHz, $CDCl_3$): $\delta=7.67$ (d, $J=8.4$ Hz, 2H), 7.52 (d, $J=8.4$ Hz, 2H), 7.52 and 7.47 (AA′XX′, $J_{AX}=8.8$ Hz, 8H), 7.50 (s, 2H), 7.37 and 6.57 (AA′XX′, $J_{AX}=8.9$ Hz, 8H), 3.28 (m, 8H), 1.98 (m, 4H), 1.58 (m, 8H), 1.32 (m, 24H), 1.30–1.02 (m, 24H), 0.91 (t, $J=6.5$ Hz, 12H), 0.82 (t, $J=6.6$ Hz, 6H), 0.61 ppm (m, 4H); ^{13}C NMR (50.32 MHz, $CDCl_3$): $\delta=151.1$, 148.0, 140.7, 132.9, 131.4, 131.1, 130.7, 125.9, 124.2, 122.0, 121.9, 120.0, 111.1, 108.4, 93.1, 91.9, 89.8, 87.0, 55.2, 50.9, 40.3, 31.8, 31.7, 30.0, 29.5, 29.3, 29.2, 27.2, 26.8, 23.7, 22.7, 22.6, 14.04, 14.02 ppm; HRMS (LSIMS$^+$, *o*NPOE): *m*/*z*: calcd for $C_{87}H_{112}N_2$ [M^+]: 1184.8826; found: 1184.8813; elemental analysis calcd (%) for $C_{87}H_{112}N_2$ (1185.86): C 88.12, H 9.52, N 2.36; found: C 88.00, H 9.65, N 2.18.

4,4′-[(9,9-Dinonyl-9*H*-fluorene-2,7-diyl)bis[2,1-ethynediyl-4,1-phenylene-(1*E*)-2,1-ethenediyl]]bis(*N*,*N*-dioctylbenzenamine) (20): Reaction of **18d** (96 mg, 0.206 mmol) with **4a** (272 mg, 0.498 mmol), as described for **13a**, for 15 h, with subsequent purification by column chromatography (heptane/CH_2Cl_2, gradient from 90:10 to 80:20), afforded 223 mg (83%) of **20**; ^{1}H NMR (200.13 MHz, $CDCl_3$): $\delta=7.66$ (d, $J=8.6$ Hz, 2H), 7.52 (d, $J=8.6$ Hz, 2H), 7.52 and 7.45 (AA′XX′, $J_{AX}=8.6$ Hz, 8H), 7.50 (s, 2H), 7.38 and 6.62 (AA′XX′, $J_{AX}=8.7$ Hz, 8H), 7.08 (d, $J=16.1$ Hz, 2H), 6.86 (d, $J=16.1$ Hz, 2H), 3.28 (m, 8H), 1.98 (m, 4H), 1.59 (m, 8H), 1.31 (m, 40H), 1.30–1.02 (m, 24H), 0.89 (t, $J=6.2$ Hz, 12H), 0.83 (t, $J=6.7$ Hz, 6H), 0.62 ppm (m, 4H); ^{13}C NMR (50.32 MHz, $CDCl_3$): $\delta=151.1$, 148.0, 140.6, 138.4, 131.8, 130.7, 129.9, 127.9, 125.8, 125.7, 124.2, 122.8, 122.1, 121.0, 119.9, 111.6, 90.9, 90.3, 55.2, 51.0, 40.4, 31.82, 31.80, 30.0, 29.52, 29.48, 29.31, 29.3, 29.2, 27.3, 27.2, 23.7, 22.64, 22.61, 14.1, 14.0 ppm; HRMS (LSIMS$^+$, *o*NPOE): *m*/*z*: calcd for $C_{95}H_{132}N_2$ [M^+]: 1301.0391; found: 1301.0381; elemental analysis calcd (%) for $C_{95}H_{132}N_2$ (1302.10): C 87.63, H 10.22, N 2.15; found: C 87.48, H 10.13, N 1.91.

9,9-Dinonyl-2,7-bis{[4-(octylsulfonyl)phenyl]ethynyl}-9*H*-fluorene (21a): Reaction of **18d** (106.7 mg, 0.229 mmol) with **8a** (174 mg, 0.523 mmol), as described for **13a**, at 45 °C for 6 h, with subsequent purification by column chromatography (heptane/CH_2Cl_2 35:65), afforded 186.0 mg (84%) of **21a**; ^{1}H NMR (200.13 MHz, $CDCl_3$): $\delta=7.91$ and 7.73 (AA′XX′, $J_{AX}=8.6$ Hz, 8H), 7.72 (d, $J=8.0$ Hz, 2H), 7.56 (d, $J=8.0$ Hz, 2H), 7.54 (s, 2H), 3.11 (m, 4H), 2.00 (m, 4H), 1.73 (m, 4H), 1.41–1.02 (m, 44H), 0.87 (t, $J=6.5$ Hz, 6H), 0.81 (t, $J=6.6$ Hz, 6H), 0.61 ppm (m, 4H); ^{13}C NMR (50.32 MHz, $CDCl_3$): $\delta=151.2$, 141.2, 138.1, 132.0, 131.0, 129.1, 128.1, 126.1, 121.1, 120.2, 94.3, 88.2, 56.3, 55.3, 40.2, 31.7, 31.6, 29.9, 29.4, 29.2, 29.1, 28.9, 28.8, 28.2, 23.7, 22.59, 22.55, 22.50, 14.02, 14.01 ppm; HRMS (LSIMS$^+$, *m*NBA): *m*/*z*: calcd for $C_{63}H_{86}O_4S_2$ [M^+]: 970.5968; found: 970.5981; elemental analysis calcd (%) for $C_{63}H_{86}O_4S_2$ (971.49): C 77.89, H 8.92; found: C 77.66, H 8.96.

9,9-Dinonyl-2,7-bis{[4-[(trifluoromethyl)sulfonyl]phenyl]ethynyl}-9*H*-fluorene (21b): Reaction of **18b** (175.7 mg, 0.26 mmol) with **8d** (153.4 mg, 0.66 mmol), as described for **13a**, at 40 °C for 14 h, with subsequent purification by column chromatography (heptane/CH_2Cl_2 80:20), afforded 138.0 mg (60%) of **21b**; ^{1}H NMR (200.13 MHz, $CDCl_3$): $\delta=8.04$ and 7.82 (AA′XX′, $J_{AX}=8.5$ Hz, 8H), 7.74 (d, $J=7.9$ Hz, 2H), 7.58 (d, $J=7.9$ Hz, 2H), 7.56 (s, 2H), 2.02 (m, 4H), 1.26–1.07 (m, 24H), 0.81 (t, $J=6.6$ Hz, 6H), 0.62 ppm (m, 4H); ^{13}C NMR (75.48 MHz, $CDCl_3$): $\delta=151.4$, 141.6, 132.5, 132.4, 131.3, 130.7, 129.9, 126.4, 120.9, 120.4, 120.2 (q, $J=325.9$ Hz), 96.7, 87.8, 55.5, 40.2, 31.8, 29.9, 29.5, 29.2, 23.7, 22.6, 14.0 ppm; ^{19}F NMR (282.38 MHz, $CDCl_3$): $\delta=-78.22$ ppm; HRMS (LSIMS$^+$, *m*NBA): *m*/*z*: calcd for $C_{49}H_{52}F_6O_4S_2$ [M^+]: 882.3211; found: 882.3225.

9,9-Dinonyl-2,7-bis{[4-[(1*E*)-2-[4-(octylsulfonyl)phenyl]ethenyl]phenyl]-ethynyl}-9*H*-fluorene (21c): Reaction of **18d** (109.7 mg, 0.235 mmol) with **10** (271 mg, 0.562 mmol), as described for **13a**, at 35 °C for 14 h, with subsequent purification by column chromatography (heptane/CH_2Cl_2 25:75 then 20:80), afforded 239.8 mg (87%) of **21c**: M.p. 164–165 °C; ^{1}H NMR (200.13 MHz, $CDCl_3$): $\delta=7.89$ and 7.68 (AA′XX′, $J_{AX}=8.6$ Hz, 8H), 7.69 (d, $J=8.0$ Hz, 2H), 7.53 (d, $J=8.0$ Hz, 2H), 7.60 and 7.54 (AA′XX′, $J_{AX}=8.8$ Hz, 8H), 7.54 (s, 2H), 7.27 (d, $J=16.5$ Hz, 2H), 7.16 (d, $J=16.5$ Hz, 2H), 3.10 (m, 4H), 2.01 (m, 4H), 1.73 (m, 4H), 1.41–1.00 (m, 44H), 0.86 (t, $J=6.4$ Hz, 6H), 0.83 (t, $J=6.7$ Hz, 6H), 0.62 ppm (m, 4H); ^{13}C NMR (50.32 MHz, $CDCl_3$): $\delta=151.1$, 142.3, 140.7, 137.6, 136.1, 131.9, 131.7, 130.8, 128.5, 127.3, 127.0, 126.8, 125.9, 123.3, 121.8, 120.0, 92.0, 89.8, 56.3, 55.2, 40.3, 31.7, 31.6, 29.9, 29.4, 29.2, 29.1, 28.9, 28.8, 28.2, 23.7, 22.6, 22.54, 22.48, 14.01, 13.98 ppm; HRMS (LSIMS$^+$, *m*NBA): *m*/*z*: calcd for $C_{79}H_{98}O_4S_2$ [M^+]: 1174.6907; found: 1174.6913; elemental analysis calcd (%) for $C_{79}H_{98}O_4S_2$ (1175.76): C 80.70, H 8.40; found: C 80.71, H 8.41.

2,7-Bis[(1*E*)-2-(4-methoxyphenyl)ethenyl]-9,9-dinonyl-9*H*-fluorene (23): *t*BuOK (87 mg, 0.77 mmol) was added to a solution of **22b** (122.0 mg, 0.26 mmol) and 4-(methoxybenzyl)triphenylphosphonium bromide[119] (261.8 mg, 0.57 mmol) in anhyd CH_2Cl_2 (5 mL). The mixture was stirred at 20 °C for 48 h. After addition of water, extraction with CH_2Cl_2, and drying (Na_2SO_4), the solvent was evaporated. The residue was purified by filtration through a short pad of silica gel (CH_2Cl_2), to afford a mixture of isomers, which was dissolved in Et_2O (5 mL). A catalytic amount of I_2 was then added and the solution was stirred at 20 °C for 3 h under light exposure (75-W lamp). The organic layer was washed with aq $Na_2S_2O_3$ and dried (Na_2SO_4). After evaporation of the solvent, the crude product was purified by column chromatography (heptane/AcOEt 98:2 then 95:5) to yield 130.7 mg (75%) of **23**; ^{1}H NMR (200.13 MHz, $CDCl_3$): $\delta=7.65$ (d, $J=7.8$ Hz, 2H), 7.51 and 6.93 (AA′XX′, $J_{AX}=8.8$ Hz, 8H), 7.48 (d, $J=7.8$ Hz, 2H), 7.46 (s, 2H), 7.16 (d, $J=16.4$ Hz, 2H), 7.07 (d, $J=16.4$ Hz, 2H), 3.85 (s, 6H), 2.02 (m, 4H), 1.27–1.08 (m, 24H), 0.82 (t, $J=6.6$ Hz, 6H), 0.69 ppm (m, 4H); ^{13}C NMR (75.48 MHz, $CDCl_3$): $\delta=159.2$, 151.4, 140.3, 136.5, 130.3, 127.6, 127.4, 127.3, 125.3, 120.4, 119.8, 114.1, 55.2, 54.9, 40.5, 31.8, 30.0, 29.5, 29.24, 29.21, 23.7, 22.6, 14.0 ppm; HRMS (ES$^+$): *m*/*z*: calcd for $C_{49}H_{62}NaO_2$ [M+Na]$^+$: 705.4647; found: 705.4640; elemental analysis calcd (%) for $C_{49}H_{62}O_2$ (683.03): C 86.17, H 9.15; found: C 85.53, H 9.14.

4,4′-[(9,9-Dinonyl-9*H*-fluorene-2,7-diyl)di-(1*E*)-2,1-ethenediyl]bis(*N*,*N*-dibutylbenzenamine) (24) and 7-[(1*E*)-2-[4-(dibutylamino)phenyl]-ethenyl]-9,9-dinonyl-9*H*-fluorene-2-carboxaldehyde (25): *t*BuOK (709 mg, 6.32 mmol) was added to a solution of **22b** (2 g, 4.21 mmol) and **3a**[94] (2.56 g, 4.21 mmol) in anhyd CH_2Cl_2 (50 mL). The mixture was stirred at 20 °C for 16 h. After addition of water, extraction with CH_2Cl_2, and

 © 2007 Wiley-VCH Verlag GmbH & Co. KGaA, Weinheim

drying (Na_2SO_4), the solvent was evaporated. The residue was filtered through a short pad of silica gel (CH_2Cl_2), to afford a mixture, which was dissolved in Et_2O (65 mL). A catalytic amount of I_2 was then added and the solution was stirred at 20 °C for 16 h under light exposure (75-W lamp). The organic layer was washed with aq $Na_2S_2O_3$ and dried (Na_2SO_4). After evaporation of the solvent, the compounds were separated by column chromatography (heptane/CH_2Cl_2, gradient from 100:0 to 70:30) to yield 430 mg (12%) of **24** and 1.68 g (59%) of **25**.

Data for **24**: M.p. 62 °C; ^{1}H NMR (200.13 MHz, $CDCl_3$): δ = 7.60 (d, J = 8.0 Hz, 2H), 7.43 (d, J = 8.0 Hz, 2H), 7.41 (s, 2H), 7.40 and 6.63 (AA′XX′, J_{AX} = 8.8 Hz, 8H), 7.09 (d, J = 16.3 Hz, 2H), 6.95 (d, J = 16.3 Hz, 2H), 3.30 (m, 8H), 1.99 (m, 4H), 1.58 (m, 8H), 1.37 (m, 8H), 1.24–1.06 (m, 24H), 0.97 (t, J = 7.2 Hz, 12H), 0.81 (t, J = 6.5 Hz, 6H), 0.69 ppm (m, 4H); ^{13}C NMR (50.32 MHz, $CDCl_3$): δ = 151.3, 147.6, 139.8, 137.0, 128.0, 127.6, 124.9, 124.7, 124.3, 120.0, 119.5, 111.6, 54.8, 50.7, 40.6, 31.8, 30.1, 29.53, 29.47, 29.2, 23.7, 22.6, 20.3, 14.05, 13.99 ppm; HRMS (LSIMS$^+$, *m*NBA): *m*/*z*: calcd for $C_{63}H_{92}N_2$ [M^+]: 876.7261; found: 876.7258.

Data for **25**: M.p. 77 °C; ^{1}H NMR (200.13 MHz, $CDCl_3$): δ = 10.04 (s, 1H), 7.85 (d, J = 1.5 Hz, 1H), 7.84 (dd, J = 8.2 Hz, 1.5, 1H), 7.78 (d, J = 8.2 Hz, 1H), 7.71 (d, J = 8.0 Hz, 1H), 7.49 (d, J = 8.0 Hz, 1H), 7.44 (s, 1H), 7.41 and 6.64 (AA′XX′, J_{AX} = 8.9 Hz, 4H), 7.14 (d, J = 16.2 Hz, 1H), 6.96 (d, J = 16.2 Hz, 1H), 3.30 (m, 4H), 2.02 (m, 4H), 1.60 (m, 4H), 1.37 (m, 4H), 1.24–1.04 (m, 24H), 0.97 (t, J = 7.2 Hz, 6H), 0.82 (t, J = 6.6 Hz, 6H), 0.62 ppm (m, 4H); ^{13}C NMR (50.32 MHz, $CDCl_3$): δ = 192.0, 152.6, 151.5, 147.8, 147.4, 139.2, 137.9, 134.8, 130.5, 129.4, 127.8, 125.1, 124.2, 123.5, 122.7, 121.0, 120.1, 119.5, 111.5, 55.0, 50.6, 40.2, 31.7, 29.8, 29.4, 29.1, 26.3, 23.6, 22.5, 20.2, 14.0. 13.9 ppm; HRMS (LSIMS$^+$, *m*NBA): *m*/*z*: calcd for $C_{48}H_{69}NO$ [M^+]: 675.5379; found: 675.5379.

2,7-Bis[(1*E*)-2-[4-(methylsulfonyl)phenyl]ethenyl]-9,9-dinonyl-9*H*-fluorene (26a): NaH (60 mg, 60% dispersion in mineral oil) was added to a solution of **22b** (237 mg, 0.499 mmol) and **9a**[98] (337 mg, 1.1 mmol) in anhyd THF (15 mL). The mixture was stirred at 20 °C for 16 h. After addition of water, extraction with CH_2Cl_2, and drying (Na_2SO_4), the solvent was evaporated. The residue was purified by filtration through a short pad of silica gel (CH_2Cl_2), to yield 370 mg (95%) of **26a**: M.p. 152–153 °C; ^{1}H NMR (200.13 MHz, $CDCl_3$): δ = 7.94 and 7.71 (AA′XX′, J_{AX} = 8.3 Hz, 8H), 7.71 (d, J = 8.2 Hz, 2H), 7.54 (d, J = 8.1 Hz, 2H), 7.51 (s, 2H), 7.36 (d, J = 16.3 Hz, 2H), 7.19 (d, J = 16.3 Hz, 2H), 3.09 (s, 6H), 2.04 (m, 4H), 1.25–1.01 (m, 24H), 0.79 (t, J = 6.6 Hz, 6H), 0.63 ppm (m, 4H); ^{13}C NMR (50.32 MHz, $CDCl_3$): δ = 151.7, 142.9, 141.2, 138.5, 135.4, 133.0, 127.8, 126.8, 126.2, 125.8, 121.1, 120.2, 55.0, 44.5, 40.3, 31.7, 29.9, 29.6, 29.4, 29.1, 23.6, 22.5, 14.0 ppm; HRMS (LSIMS$^+$, *m*NBA): *m*/*z*: calcd for $C_{49}H_{62}O_4S_2$ [M^+]: 778.4090; found: 778.4096.

2,7-Bis[(1*E*)-2-[4-[(1*E*)-2-[4-(methylsulfonyl)phenyl]ethenyl]phenyl]ethenyl]-9,9-dinonyl-9*H*-fluorene (26b): NaH (18 mg, 60% dispersion in mineral oil) was added to a solution of **22b** (66.5 mg, 0.14 mmol) and **11** (115 mg, 0.28 mmol) in anhyd THF (10 mL). The mixture was stirred at 20 °C for 16 h and the solvent was removed under reduced pressure. After addition of water, extraction with CH_2Cl_2, and drying (Na_2SO_4), the solvent was evaporated. The residue was purified by column chromatography (CH_2Cl_2) to yield 87 mg (63%) of **26b**; ^{1}H NMR (200.13 MHz, $CDCl_3$): δ = 7.93 and 7.70 (AA′XX′, J_{AX} = 8.5 Hz, 8H), 7.69 (d, J = 8.8 Hz, 2H), 7.58 (m, 8H), 7.52 (d, J = 8.8 Hz, 2H), 7.49 (s, 2H), 7.26 (d, J = 16.3 Hz, 2H), 7.25 (s, 4H), 7.16 (d, J = 16.3 Hz, 2H), 3.08 (s, 6H), 2.02 (m, 4H), 1.24–1.07 (m, 24H), 0.81 (t, J = 6.7 Hz, 6H), 0.67 ppm (m, 4H); HRMS (LSIMS$^+$, *m*NBA): *m*/*z*: calcd for $C_{65}H_{74}O_4S_2$ [M^+]: 982.5029; found: 982.4992.

4,4′-[(9,9-Dinonyl-9*H*-fluorene-2,7-diyl)di-(1*E*)-2,1-ethenediyl]dibenzenamine (28): Air was removed from a solution of **27** (65.9 mg, 0.14 mmol), 4-iodoaniline (**1a**) (77.0 mg, 0.35 mmol), and K_2CO_3 (49.9 mg, 0.36 mmol) in anhyd DMF (3 mL) by blowing argon for 30 min. Then nBu$_4$NCl (103.9 mg, 0.37 mmol), PPh_3 (7.5 mg, 0.029 mmol) and $Pd(OAc)_2$ (3.2 mg, 0.014 mmol) were added. Thereafter, the mixture was stirred at 90 °C for 22 h. The solvent was removed by distillation, and the crude product was purified by column chromatography (heptane/CH_2Cl_2 30:70 then 25:75) to yield 51.0 mg (56%) of **28**; ^{1}H NMR (200.13 MHz, $CDCl_3$): δ = 7.62 (d, J = 7.9 Hz, 2H), 7.44 (d, J = 7.9 Hz, 2H), 7.42 (s, 2H), 7.38 and 6.70 (AA′XX′, J_{AX} = 8.5 Hz, 8H), 7.10 (d, J = 16.4 Hz, 2H), 7.00 (d, J = 16.4 Hz, 2H), 3.68 (br s, 4H), 2.03 (m, 4H), 1.30–1.10 (m, 24H), 0.87 (t, 6H), 0.70 ppm (m, 4H); ^{13}C NMR (75.48 MHz, $CDCl_3$): δ = 151.4, 145.9, 140.1, 136.7, 128.4, 127.8, 127.7, 125.8, 125.2, 120.3, 119.7, 115.3, 54.9, 40.6, 31.8, 30.1, 29.5, 29.2, 23.8, 22.8, 22.6, 14.0 ppm; HRMS (LSIMS$^+$, *m*NBA): *m*/*z*: calcd for $C_{47}H_{60}N_2$ [M^+]: 652.4756; found: 652.4733.

4,4′-[(9,9-Dinonyl-9*H*-fluorene-2,7-diyl)bis[(1*E*)-2,1-ethenediyl-4,1-phenylene-(1*E*)-2,1-ethenediyl]]bis(*N*,*N*-dihexylbenzenamine) (30): NaH (15 mg, 60% dispersion in mineral oil) was added to a solution of **29c** (124.4 mg, 0.17 mmol) and **4b** (149.1 mg, 0.38 mmol) in anhyd THF (9 mL). The mixture was stirred at 20 °C for 20 h and the solvent was removed under reduced pressure. After addition of water, extraction with CH_2Cl_2, and drying (Na_2SO_4), the solvents were evaporated. The residue was purified by column chromatography (heptane/CH_2Cl_2 80:20) to yield 82.0 mg (53%) of **30**; ^{1}H NMR (300.13 MHz, $CDCl_3$): δ = 7.62 (d, J = 8.3 Hz, 2H), 7.57–7.50 (m, 12H), 7.42 (d, J = 8.7 Hz, 4H), 7.25 (d, J = 16.3 Hz, 2H), 7.17 (d, J = 16.3 Hz, 2H), 7.10 (d, J = 16.2 Hz, 2H), 6.93 (d, J = 16.2 Hz, 2H), 6.66 (d, J = 8.7 Hz, 4H), 3.32 (m, 8H), 2.07 (m, 4H), 1.64 (m, 8H), 1.37 (m, 24H), 1.18–1.10 (m, 24H), 0.96 (t, J = 6.4 Hz, 12H), 0.85 (t, J = 6.9 Hz, 6H), 0.75 ppm (m, 4H); ^{13}C NMR (75.48 MHz, $CDCl_3$): δ = 151.5, 147.8, 140.5, 137.6, 136.4, 135.7, 128.8, 128.5, 127.8, 127.7, 126.7, 126.2, 125.5, 124.5, 123.2, 120.7, 120.0, 111.6, 55.0, 51.0, 40.5, 31.8, 31.7, 30.1, 29.5, 29.24, 29.22, 27.3, 26.8, 23.8, 22.7, 22.6, 14.0 ppm; HRMS (ES$^+$): *m*/*z*: calcd for $C_{87}H_{121}N_2$ [M+H]$^+$: 1193.9530; found: 1193.9502.

4,4′-[(9,9-Dinonyl-9*H*-fluorene-2,7-diyl)bis[(1*E*)-2,1-ethenediyl-5,2-thiophenediyl-(1*E*)-2,1-ethenediyl]]bis(*N*,*N*-dioctylbenzenamine) (31): NaH (48 mg, 60% dispersion in mineral oil) was added to a solution of **29c** (140.5 mg, 0.195 mmol), **6b** (225 mg, 0.496 mmol), and [18]crown-6 (10 mg) in anhyd THF (20 mL). The mixture was refluxed for 7 h. After addition of water, extraction with CH_2Cl_2, and drying (Na_2SO_4), the solvents were evaporated. The residue was then purified by column chromatography (heptane/CH_2Cl_2 90:10) to yield 175 mg (68%) of **31**; ^{1}H NMR (200.13 MHz, $CDCl_3$): δ = 7.63 (d, J = 8.1 Hz, 2H), 7.43 (d, J = 8.1 Hz, 2H), 7.41 (s, 2H), 7.33 and 6.61 (AA′XX′, J_{AX} = 8.9 Hz, 8H), 7.24 (d, J = 15.9 Hz, 2H), 6.97 (d, J = 15.6 Hz, 2H), 6.95 (d, J = 15.9 Hz, 2H), 6.94 (d, J = 3.9 Hz, 2H), 6.86 (d, J = 3.9 Hz, 2H), 6.83 (d, J = 15.6 Hz, 2H), 3.28 (m, 8H), 2.00 (m, 4H), 1.59 (m, 8H), 1.30 (m, 40H), 1.15–1.07 (m, 24H), 0.89 (t, J = 6.5 Hz, 12H), 0.82 (t, J = 6.7 Hz, 6H), 0.67 ppm (m, 4H); ^{13}C NMR (50.32 MHz, $CDCl_3$): δ = 151.5, 147.8, 143.2, 140.6, 140.5, 136.1, 129.1, 128.3, 127.7, 127.0, 125.4, 125.3, 124.0, 121.4, 120.4, 119.9, 117.0, 111.6, 54.9, 51.0, 31.8, 30.0, 29.53, 29.50, 29.33, 29.26, 29.23, 27.3, 27.2, 22.65, 22.62, 14.10, 14.07 ppm; HRMS (LSIMS$^+$, *m*NBA): *m*/*z*: calcd for $C_{91}H_{132}N_2S_2$ [M^+]: 1316.9832; found: 1316.9837; elemental analysis calcd (%) for $C_{91}H_{132}N_2S_2$ (1318.18): C 82.92, H 10.09, N 2.12, S 4.86; found: C 82.82, H 10.33, N 2.07, S 4.83.

4,4′-[(9,9-Dinonyl-9*H*-fluorene-2,7-diyl)bis[(1*E*)-2,1-ethenediyl-7,2-(9,9-dinonyl-9*H*-fluorenediyl)-(1*E*)-2,1-ethenediyl]]bis(*N*,*N*-dibutylbenzenamine) (32): NaH (25 mg, 60% dispersion in mineral oil) was added to a solution of **29c** (200 mg, 0.278 mmol) and **25** (414 mg, 0.612 mmol) in anhyd THF (15 mL). The mixture was stirred at 20 °C for 16 h and the solvent was removed under reduced pressure. After addition of water, extraction with CH_2Cl_2, and drying (Na_2SO_4), the solvent was evaporated. The residue was purified by column chromatography (heptane/CH_2Cl_2, gradient from 92:8 to 85:15) to yield 410 mg (84%) of **32**; ^{1}H NMR (300.13 MHz, $CDCl_3$): δ = 7.66 (d, J = 7.6 Hz, 2H), 7.64 (s, 2H), 7.63 (d, J = 7.6 Hz, 2H), 7.53 (d, J = 8.4 Hz, 2H), 7.52 (s, 2H), 7.52 (d, J = 8.0 Hz, 2H), 7.51 (s, 2H), 7.45 and 6.64 (AA′XX′, J_{AX} = 8.8 Hz, 8H), 7.41 (d, J = 8.2 Hz, 4H), 7.27 (s, 4H), 7.10 (d, J = 16.1 Hz, 2H), 6.97 (d, J = 16.1 Hz, 2H), 3.30 (m, 8H), 2.02 (m, 12H), 1.60 (m, 8H), 1.37 (m, 8H), 1.22–1.07 (m, 72H), 0.97 (t, J = 7.3 Hz, 12H), 0.81 (t, J = 6.8 Hz, 18H), 0.68 ppm (m, 12H); ^{13}C NMR (75.48 MHz, $CDCl_3$): δ = 151.5, 151.4, 147.7, 140.8, 140.5, 139.6, 137.3, 136.5, 136.1, 128.6, 128.2, 127.7, 125.7, 125.0, 124.7, 124.3, 120.5, 120.1, 119.8, 111.6, 55.0, 54.9, 50.8, 40.7, 31.7, 30.1, 29.5, 29.3, 29.2, 23.8, 22.6, 20.3, 14.1, 14.0 ppm; HRMS (ES$^+$, CH_2Cl_2/MeOH): *m*/*z*: calcd for $C_{129}H_{185}N_2$ [M+H]$^+$: 1762.4538; found: 1762.4533; elemental analysis calcd (%) for $C_{129}H_{184}N_2$ (1762.89): C 87.89, H 10.52, N 1.59; found: C 88.05, H 10.35, N 1.31.

 © 2007 Wiley-VCH Verlag GmbH & Co. KGaA, Weinheim

1,1′-[(9,9-Dinonyl-9*H*-fluorene-2,7-diyl)bis[(1*E*)-2,1-ethenediyl-5,2-thiophenediyl]]bis(piperidine) (34a): *t*BuOK (92 mg, 0.82 mmol) was added to a solution of **22b** (129.6 mg, 0.27 mmol) and {[5-(1-piperidinyl)-2-thienyl]methyl}triphenylphosphonium iodide (357.6 mg, 0.63 mmol) in anhyd CH_2Cl_2 (4 mL). The mixture was stirred at 20 °C for 48 h. After addition of water, extraction with CH_2Cl_2, and drying (Na_2SO_4), the solvent was evaporated. The residue was purified by filtration through a short pad of silica gel (heptane/CH_2Cl_2 50:50), to afford a mixture of isomers, which was dissolved in Et_2O (5 mL). A catalytic amount of I_2 was then added and the solution was stirred at 20 °C for 3 h under light exposure (75-W lamp). The organic layer was washed with aq $Na_2S_2O_3$ and dried (Na_2SO_4). After evaporation of the solvent, the crude product was purified by column chromatography (heptane/AcOEt 99:1 then 99:2) to yield 48.5 mg (22%) of **34a**; ^{1}H NMR (200.13 MHz, $CDCl_3$): δ = 7.64 (d, J = 7.9 Hz, 2H), 7.49 (d, J = 7.9 Hz, 2H), 7.41 (s, 2H), 7.21 (d, J = 16.5 Hz, 2H), 7.18 (d, J = 5.7 Hz, 2H), 6.97 (d, J = 16.5 Hz, 2H), 6.92 (d, J = 5.7 Hz, 2H), 2.97 (m, 8H), 1.98 (m, 4H), 1.78 (m, 8H), 1.59 (m, 4H), 1.25–1.07 (m, 24H), 0.81 (t, J = 6.6 Hz, 6H), 0.72 ppm (m, 4H); ^{13}C NMR (50.32 MHz, $CDCl_3$): δ = 156.4, 151.5, 140.1, 136.9, 127.3, 127.2, 124.8, 124.1, 120.8, 120.7, 119.7, 117.2, 56.3, 54.8, 40.4, 31.8, 30.1, 29.6, 29.3, 29.2, 26.1, 23.9, 22.6, 14.1 ppm; HRMS (LSIMS$^+$, *m*NBA): *m*/*z*: calcd for $C_{53}H_{72}N_2S_2$ [M^+]: 800.5137; found: 800.5149; elemental analysis calcd (%) for $C_{53}H_{72}N_2S_2$ (801.30): C 79.44, H 9.06, N 3.50, S 8.00; found: C 79.66, H 9.42, N 3.22, S 7.70.

1,1′-[(9,9-Dinonyl-9*H*-fluorene-2,7-diyl)bis[(1*E*)-2,1-ethenediyl-5,2-thiophenediyl-(1*E*)-2,1-ethenediyl-5,2-thiophenediyl]]bis(piperidine) (34b): Reaction of **33** (77.0 mg, 0.11 mmol) with {[5-(1-piperidinyl)-2-thienyl]-methyl}triphenylphosphonium iodide (140.0 mg, 0.25 mmol), as described for **34a**, with subsequent purification by column chromatography (heptane/CH_2Cl_2, gradient from 70:30 to 40:60), afforded 20.2 mg (18%) of **34b**; ^{1}H NMR (300.13 MHz, $CDCl_3$): δ = 7.64 (d, J = 8.0 Hz, 2H), 7.45 (d, J = 8.0 Hz, 2H), 7.41 (s, 2H), 7.25 (d, J = 15.9 Hz, 2H), 7.08 (d, J = 5.4 Hz, 2H), 6.99 (d, J = 15.9 Hz, 2H), 6.98 (s, 4H), 6.96 (d, J = 3.8 Hz, 2H) 6.89 (d, J = 3.8 Hz, 2H), 6.85 (d, J = 5.4 Hz, 2H), 2.95 (m, 8H), 2.00 (m, 4H), 1.80 (m, 8H), 1.59 (m, 4H), 1.26–1.05 (m, 24H), 0.82 (t, J = 6.8 Hz, 6H), 0.66 ppm (m, 4H); ^{13}C NMR (75.48 MHz, $CDCl_3$): δ = 156.8, 151.6, 142.9, 141.4, 140.6, 136.0, 128.7, 127.0, 126.6, 126.1, 125.4, 123.9, 121.6, 121.3, 120.5, 120.0, 119.9, 116.4, 56.3, 55.0, 40.6, 31.8, 30.1, 29.5, 29.3, 29.2, 26.2, 23.9, 23.8, 22.6, 14.1 ppm; HRMS (ES$^+$, MeOH): *m*/*z*: calcd for $C_{65}H_{81}N_2S_4$ [M+H]$^+$: 1017.5283; found: 1017.5268.

Acknowledgements

We acknowledge financial support from Rennes Métropole and Délégation Générale pour l'Armement (DGA Grant 00.34.070.00.470.75.653). L.P. and M.C. received fellowships from MENESR and DGA, respectively. We wish to thank M. H. V. Werts for important help in TPEF experiments, B. K. G. Bhatthula, K. Rousseau, A. Le Cornec, and D. Béret for assistance in the synthesis.

[1] R. R. Birge, *Acc. Chem. Res.* **1986**, *19*, 138–146.
[2] S. Shima, R. P. Ilagan, N. Gillespie, B. J. Sommer, R. G. Hiller, F. P. Sharples, H. A. Frank, R. R. Birge, *J. Phys. Chem. A* **2003**, *107*, 8052–8066.
[3] D. A. Parthenopoulos, P. M. Rentzepis, *Science* **1989**, *245*, 843–845.
[4] J. H. Strickler, W. W. Webb, *Opt. Lett.* **1991**, *16*, 1780–1782.
[5] A. S. Dvornikov, P. M. Rentzepis, *Opt. Commun.* **1995**, *119*, 341–346.
[6] K. D. Belfield, K. J. Schafer, *Chem. Mater.* **2002**, *14*, 3656–3662.
[7] K. D. Belfield, Y. Liu, R. A. Negres, M. Fan, G. Pan, D. J. Hagan, F. E. Hernandez, *Chem. Mater.* **2002**, *14*, 3663–3667.
[8] S. Maruo, O. Nakamura, S. Kawata, *Opt. Lett.* **1997**, *22*, 132–134.
[9] B. H. Cumpston, S. P. Ananthavel, S. Barlow, D. L. Dyer, J. E. Ehrlich, L. L. Erskine, A. A. Heikal, S. M. Kuebler, I.-Y. S. Lee, D. McCord-Maughon, J. Qin, H. Röckel, M. Rumi, X. L. Wu, S. R. Marder, J. W. Perry, *Nature* **1999**, *398*, 51–54.
[10] S. Kawata, H.-B. Sun, T. Tanaka, K. Takada, *Nature* **2001**, *412*, 697–698.
[11] W. Zhou, S. M. Kuebler, K. L. Braun, T. Yu, J. K. Cammack, C. K. Ober, J. W. Perry, S. R. Marder, *Science* **2002**, *296*, 1106–1109.
[12] J. D. Bhawalkar, G. S. He, C.-K. Park, C. F. Zhao, G. Ruland, P. N. Prasad, *Opt. Commun.* **1996**, *124*, 33–37.
[13] A. Abbotto, L. Beverina, R. Bozio, S. Bradamante, C. Ferrante, G. A. Pagani, R. Signorini, *Adv. Mater.* **2000**, *12*, 1963–1967.
[14] W. Denk, J. H. Strickler, W. W. Webb, *Science* **1990**, *248*, 73–76.
[15] C. Xu, W. Zipfel, J. B. Shear, R. M. Williams, W. W. Webb, *Proc. Natl. Acad. Sci. USA* **1996**, *93*, 10763–10768.
[16] D. R. Larson, W. R. Zipfel, R. M. Williams, S. W. Clark, M. P. Bruchez, F. W. Wise, W. W. Webb, *Science* **2003**, *300*, 1434–1437.
[17] W. Denk, P. B. Detwiler, *Proc. Natl. Acad. Sci. USA* **1999**, *96*, 7035–7040.
[18] J. D. Bhawalkar, N. D. Kumar, C. F. Zhao, P. N. Prasad, *J. Clin. Laser Med. Surg.* **1997**, *15*, 201–204.
[19] D. W. Piston, M. S. Kirby, H. Cheng, W. J. Lederer, W. W. Webb, *Appl. Opt.* **1994**, *33*, 662–669.
[20] S. Charpak, J. Mertz, E. Beaurepaire, L. Moreaux, K. Delaney, *Proc. Natl. Acad. Sci. USA* **2001**, *98*, 1230–1234.
[21] M. Wachowiak, W. Denk, W. Friedrich Rainer, *Proc. Natl. Acad. Sci. USA* **2004**, *101*, 9097–9102.
[22] M. Taki, J. L. Wolford, T. V. O'Halloran, *J. Am. Chem. Soc.* **2004**, *126*, 712–713.
[23] C. J. Chang, E. M. Nolan, J. Jaworski, K. Okamoto, Y. Hayashi, M. Sheng, S. J. Lippard, *Inorg. Chem.* **2004**, *43*, 6774–6779.
[24] W. R. Zipfel, R. M. Williams, R. Christie, A. Y. Nikitin, B. T. Hyman, W. W. Webb, *Proc. Natl. Acad. Sci. USA* **2003**, *100*, 7075–7080.
[25] Y. P. Meshalkin, *Kvantovaya Elektron.* **1996**, *23*, 551–552.
[26] G. F. White, K. L. Litvinenko, S. R. Meech, D. L. Andrews, A. J. Thomson, *Photochem. Photobiol. Sci.* **2004**, *3*, 47–55.
[27] G. S. He, G. C. Xu, P. N. Prasad, B. A. Reinhardt, J. C. Bhatt, R. McKellar, A. G. Dillard, *Opt. Lett.* **1995**, *20*, 435–437.
[28] G. S. He, J. D. Bhawalkar, C. F. Zhao, P. N. Prasad, *Appl. Phys. Lett.* **1995**, *67*, 2433–2435.
[29] J. E. Ehrlich, X. L. Wu, I. Y. S. Lee, A. A. Heikal, Z. Y. Hu, H. Röckel, S. R. Marder, J. W. Perry, *Mater. Res. Soc. Symp. Proc.* **1997**, *479*, 9–15.
[30] J. E. Ehrlich, X. L. Wu, I. Y. S. Lee, Z. Y. Hu, H. Röckel, S. R. Marder, J. W. Perry, *Opt. Lett.* **1997**, *22*, 1843–1845.
[31] J. W. Perry, S. Barlow, J. E. Ehrlich, A. A. Heikal, Z. Y. Hu, I. Y. Lee, K. Mansour, S. R. Marder, H. Röckel, M. Rumi, S. Thayumanavan, X. L. Wu, *Nonlinear Opt.* **1999**, *21*, 225–243.
[32] Y. Morel, A. Irimia, P. Najechalski, Y. Kervella, O. Stephan, P. L. Baldeck, C. Andraud, *J. Chem. Phys.* **2001**, *114*, 5391–5396.
[33] R. Anémian, Y. Morel, P. L. Baldeck, B. Paci, K. Kretsch, J.-M. Nunzi, C. Andraud, *J. Mater. Chem.* **2003**, *13*, 2157–2163.
[34] K.-S. Lee, H.-K. Yang, J.-H. Lee, O.-K. Kim, H. Y. Woo, H. Choi, M. Cha, M. Blanchard-Desce, *Proc. SPIE-Int. Soc. Opt. Eng.* **2003**, *4991*, 175–182.
[35] M. G. Silly, L. Porrès, O. Mongin, P.-A. Chollet, M. Blanchard-Desce, *Chem. Phys. Lett.* **2003**, *379*, 74–80.
[36] D. Riehl, N. Izard, L. Vivien, E. Anglaret, E. Doris, C. Ménard, C. Mioskowski, L. Porrès, O. Mongin, M. Charlot, M. Blanchard-Desce, R. Anémian, J.-C. Mulatier, C. Barsu, C. Andraud, *Proc. SPIE-Int. Soc. Opt. Eng.* **2003**, *5211*, 124–134.
[37] N. Izard, C. Menard, D. Riehl, E. Doris, C. Mioskowski, E. Anglaret, *Chem. Phys. Lett.* **2004**, *391*, 124–128.
[38] C. Li, C. Liu, Q. Li, Q. Gong, *Chem. Phys. Lett.* **2004**, *400*, 569–572.
[39] M. Charlot, N. Izard, O. Mongin, D. Riehl, M. Blanchard-Desce, *Chem. Phys. Lett.* **2006**, *417*, 297–302.
[40] O. Mongin, L. Porrès, L. Moreaux, J. Mertz, M. Blanchard-Desce, *Org. Lett.* **2002**, *4*, 719–722.
[41] M. Albota, D. Beljonne, J.-L. Brédas, J. E. Ehrlich, J.-Y. Fu, A. A. Heikal, S. E. Hess, T. Kogej, M. D. Levin, S. R. Marder, D.

 © 2007 Wiley-VCH Verlag GmbH & Co. KGaA, Weinheim

McCord-Maughon, J. W. Perry, H. Röckel, M. Rumi, G. Subramaniam, W. W. Webb, X.-L. Wu, C. Xu, *Science* **1998**, *281*, 1653–1656.
[42] M. Rumi, J. E. Ehrlich, A. A. Heikal, J. W. Perry, S. Barlow, Z.-Y. Hu, D. McCord-Maughon, T. C. Parker, H. Röckel, S. Thayumanavan, S. R. Marder, D. Beljonne, J.-L. Brédas, *J. Am. Chem. Soc.* **2000**, *122*, 9500–9510.
[43] L. Ventelon, L. Moreaux, J. Mertz, M. Blanchard-Desce, *Chem. Commun.* **1999**, 2055–2056.
[44] L. Ventelon, S. Charier, L. Moreaux, J. Mertz, M. Blanchard-Desce, *Angew. Chem.* **2001**, *113*, 2156–2159; *Angew. Chem. Int. Ed.* **2001**, *40*, 2098–2101.
[45] M. H. V. Werts, S. Gmouh, O. Mongin, T. Pons, M. Blanchard-Desce, *J. Am. Chem. Soc.* **2004**, *126*, 16294–16295.
[46] B. A. Reinhardt, L. L. Brott, S. J. Clarson, A. G. Dillard, J. C. Bhatt, R. Kannan, L. Yuan, G. S. He, P. N. Prasad, *Chem. Mater.* **1998**, *10*, 1863–1874.
[47] O.-K. Kim, K.-S. Lee, H. Y. Woo, K.-S. Kim, G. S. He, J. Swiatkiewicz, P. N. Prasad, *Chem. Mater.* **2000**, *12*, 284–286.
[48] L. Ventelon, Y. Morel, P. Baldeck, L. Moreaux, J. Mertz, M. Blanchard-Desce, *Nonlinear Opt.* **2001**, *27*, 249–258.
[49] P. K. Frederiksen, M. Jørgensen, P. R. Ogilby, *J. Am. Chem. Soc.* **2001**, *123*, 1215–1221.
[50] L. Ventelon, L. Moreaux, J. Mertz, M. Blanchard-Desce, *Synth. Met.* **2002**, *127*, 17–21.
[51] S. J. K. Pond, M. Rumi, M. D. Levin, T. C. Parker, D. Beljonne, M. W. Day, J.-L. Brédas, S. R. Marder, J. W. Perry, *J. Phys. Chem. A* **2002**, *106*, 11470–11480.
[52] A. Abbotto, L. Beverina, R. Bozio, A. Facchetti, C. Ferrante, G. A. Pagani, D. Pedron, R. Signorini, *Org. Lett.* **2002**, *4*, 1495–1498.
[53] M. Blanchard-Desce, *C. R. Phys.* **2002**, *3*, 439–448.
[54] L. Zheng, T. Sassa, A. K. Y. Jen, *Mater. Res. Soc. Symp. Proc.* **2002**, *725*, 219–224.
[55] O. Mongin, J. Brunel, L. Porrès, M. Blanchard-Desce, *Tetrahedron Lett.* **2003**, *44*, 2813–2816.
[56] B. Strehmel, A. M. Sarker, H. Detert, *ChemPhysChem* **2003**, *4*, 249–259.
[57] W. J. Yang, D. Y. Kim, M.-Y. Jeong, H. M. Kim, S.-J. Jeon, B. R. Cho, *Chem. Commun.* **2003**, 2618–2619.
[58] J. Yoo, S. K. Yang, M.-Y. Jeong, H. C. Ahn, S.-J. Jeon, B. R. Cho, *Org. Lett.* **2003**, *5*, 645–648.
[59] O. K. Kim, K. S. Lee, Z. Huang, W. B. Heuer, C. S. Paik-Sung, *Opt. Mater.* **2003**, *21*, 559–564.
[60] N. N. P. Moonen, R. Gist, C. Boudon, J.-P. Gisselbrecht, P. Seiler, T. Kawai, A. Kishioka, M. Gross, M. Irie, F. Diederich, *Org. Biomol. Chem.* **2003**, *1*, 2032–2034.
[61] M. Halik, W. Wenseleers, C. Grasso, F. Stellacci, E. Zojer, S. Barlow, J.-L. Bredas, J. W. Perry, S. R. Marder, *Chem. Commun.* **2003**, 1490–1491.
[62] Y. Iwase, K. Kamada, K. Ohta, K. Kondo, *J. Mater. Chem.* **2003**, *13*, 1575–1581.
[63] D. X. Cao, Z. Q. Liu, Q. Fang, G. B. Xu, G. Xue, G. Q. Liu, W. T. Yu, *J. Organomet. Chem.* **2004**, *689*, 2201–2206.
[64] W. J. Yang, C. H. Kim, M.-Y. Jeong, S. K. Lee, M. J. Piao, S.-J. Jeon, B. R. Cho, *Chem. Mater.* **2004**, *16*, 2783–2789.
[65] L. Porrès, C. Katan, O. Mongin, T. Pons, J. Mertz, M. Blanchard-Desce, *J. Mol. Struct.* **2004**, *704*, 17–24.
[66] G. Xia, P. Lu, X. Xu, G. Xu, *Opt. Mater.* **2004**, *27*, 109–113.
[67] Z.-Q. Liu, Q. Fang, D.-X. Cao, D. Wang, G.-B. Xu, *Org. Lett.* **2004**, *6*, 2933–2936.
[68] J. Kawamata, M. Akiba, T. Tani, A. Harada, Y. Inagaki, *Chem. Lett.* **2004**, *33*, 448–449.
[69] K. D. Belfield, A. R. Morales, B.-S. Kang, J. M. Hales, D. J. Hagan, E. W. Van Stryland, V. M. Chapela, J. Percino, *Chem. Mater.* **2004**, *16*, 4634–4641.
[70] S. J. K. Pond, O. Tsutsumi, M. Rumi, O. Kwon, E. Zojer, J.-L. Brédas, S. R. Marder, J. W. Perry, *J. Am. Chem. Soc.* **2004**, *126*, 9291–9306.
[71] H. M. Kim, M.-Y. Jeong, H. C. Ahn, S.-J. Jeon, B. R. Cho, *J. Org. Chem.* **2004**, *69*, 5749–5751.
[72] S.-i. Kato, T. Matsumoto, T. Ishi-i, T. Thiemann, M. Shigeiwa, H. Gorohmaru, S. Maeda, Y. Yamashita, S. Mataka, *Chem. Commun.* **2004**, 2342–2343.
[73] L. Porrès, O. Mongin, C. Katan, M. Charlot, B. K. G. Bhatthula, T. Pons, J. Mertz, M. Blanchard-Desce, *J. Nonlinear Opt. Phys. Mater.* **2004**, *13*, 451–460.
[74] G. P. Bartholomew, M. Rumi, S. J. K. Pond, J. W. Perry, S. Tretiak, G. C. Bazan, *J. Am. Chem. Soc.* **2004**, *126*, 11529–11542.
[75] S. K. Lee, W. J. Yang, J. J. Choi, C. H. Kim, S.-J. Jeon, B. R. Cho, *Org. Lett.* **2005**, *7*, 323–326.
[76] M. Charlot, L. Porres, C. D. Entwistle, A. Beeby, T. B. Marder, M. Blanchard-Desce, *Phys. Chem. Chem. Phys.* **2005**, *7*, 600–606.
[77] S.-J. Chung, M. Rumi, V. Alain, S. Barlow, J. W. Perry, S. R. Marder, *J. Am. Chem. Soc.* **2005**, *127*, 10844–10845.
[78] H. Y. Woo, J. W. Hong, B. Liu, A. Mikhailovsky, D. Korystov, G. C. Bazan, *J. Am. Chem. Soc.* **2005**, *127*, 820–821.
[79] H. Y. Woo, B. Liu, B. Kohler, D. Korystov, A. Mikhailovsky, G. C. Bazan, *J. Am. Chem. Soc.* **2005**, *127*, 14721–14729.
[80] G. S. He, L. Yuan, N. Cheng, J. D. Bhawalkar, P. N. Prasad, L. L. Brott, S. J. Clarson, B. A. Reinhardt, *J. Opt. Soc. Am. B* **1997**, *14*, 1079–1087.
[81] K. D. Belfield, D. J. Hagan, E. W. Van Stryland, K. J. Schafer, R. A. Negres, *Org. Lett.* **1999**, *1*, 1575–1578.
[82] K. D. Belfield, K. J. Schafer, W. Mourad, B. A. Reinhardt, *J. Org. Chem.* **2000**, *65*, 4475–4481.
[83] R. Kannan, G. S. He, L. Yuan, F. Xu, P. N. Prasad, A. G. Dombroskie, B. A. Reinhardt, J. W. Baur, R. A. Vaia, L.-S. Tan, *Chem. Mater.* **2001**, *13*, 1896–1904.
[84] L. Antonov, K. Kamada, K. Ohta, F. S. Kamounah, *Phys. Chem. Chem. Phys.* **2003**, *5*, 1193–1197.
[85] P. Audebert, K. Kamada, K. Matsunaga, K. Ohta, *Chem. Phys. Lett.* **2003**, *367*, 62–71.
[86] Z.-q. Liu, Q. Fang, D. Wang, D.-x. Cao, G. Xue, W.-t. Yu, H. Lei, *Chem. Eur. J.* **2003**, *9*, 5074–5084.
[87] S. Charier, O. Ruel, J.-B. Baudin, D. Alcor, J.-F. Allemand, A. Meglio, L. Jullien, *Angew. Chem.* **2004**, *116*, 4889–4892; *Angew. Chem. Int. Ed.* **2004**, *43*, 4785–4788.
[88] Y. Wang, O. Y. H. Tai, C. H. Wang, A. K. Y. Jen, *J. Chem. Phys.* **2004**, *121*, 7901–7907.
[89] M. Barzoukas, M. Blanchard-Desce, *J. Chem. Phys.* **2000**, *113*, 3951–3959.
[90] M. Barzoukas, M. Blanchard-Desce, *Nonlinear Opt.* **2001**, *27*, 209–218.
[91] W.-H. Lee, M. Cho, S.-J. Jeon, B. R. Cho, *J. Phys. Chem. A* **2000**, *104*, 11033–11040.
[92] C. Käpplinger, R. Beckert, *Synthesis* **2002**, 1843–1850.
[93] H. Meier, R. Petermann, U. Dullweber, *J. prakt. Chem.* **1998**, *340*, 744–754.
[94] L. Porrès, B. K. G. Bhatthula, M. Blanchard-Desce, *Synthesis* **2003**, 1541–1544.
[95] B. L. Feringa, R. Hulst, R. Rikers, L. Brandsma, *Synthesis* **1988**, 316–318.
[96] A. J. Carpenter, D. J. Chadwick, *Tetrahedron* **1985**, *41*, 3803–3812.
[97] N. Nemoto, J. Abe, F. Miyata, Y. Shirai, Y. Nagase, *J. Mater. Chem.* **1998**, *8*, 1193–1197.
[98] A. Ulman, C. S. Willand, W. Köhler, D. R. Robello, D. J. Williams, L. Handley, *J. Am. Chem. Soc.* **1990**, *112*, 7083–7090.
[99] M. S. Wong, Z. H. Li, C. C. Kwok, *Tetrahedron Lett.* **2000**, *41*, 5719–5723.
[100] S. Takahashi, Y. Kuroyama, K. Sonogashira, N. Hagihara, *Synthesis* **1980**, 627–630.
[101] A. Helms, D. Heiler, G. McLendon, *J. Am. Chem. Soc.* **1992**, *114*, 6227–6238.
[102] T. Jeffery, *Tetrahedron* **1996**, *52*, 10113–10130.
[103] We note that this reduction is not observed in the case of pull–pull systems.
[104] Although no clear phosphorescence could be observed for compound **31** in methylcyclohexane at 77 K, it has a reasonable quantum yield for the generation of singlet oxygen (0.15 in $CHCl_3$), in-

 © 2007 Wiley-VCH Verlag GmbH & Co. KGaA, Weinheim

dicating the formation of triplet states upon excitation (M. H. V. Werts, C. Frochot, unpublished data).
[105] Field contribution to the Hammett constant for phenyl: $F=0.12$; C. Hansch, A. Leo, R. W. Taft, *Chem. Rev.* **1991**, *91*, 165–195.
[106] Resonance contribution to the Hammett constant for phenyl: $R=-0.13$.
[107] C. Xu, W. W. Webb, *J. Opt. Soc. Am. B* **1996**, *13*, 481–491.
[108] D. A. Oulianov, I. V. Tomov, A. S. Dvornikov, P. M. Rentzepis, *Opt. Commun.* **2001**, *191*, 235–243.
[109] H. Rath, J. Sankar, V. PrabhuRaja, T. K. Chandrashekar, A. Nag, D. Goswami, *J. Am. Chem. Soc.* **2005**, *127*, 11608–11609.
[110] R. Misra, R. Kumar, T. K. Chandrashekar, A. Nag, D. Goswami, *Org. Lett.* **2006**, *8*, 629–631.
[111] D. Y. Kim, T. K. Ahn, J. H. Kwon, D. Kim, T. Ikeue, N. Aratani, A. Osuka, M. Shigeiwa, S. Maeda, *J. Phys. Chem. A* **2005**, *109*, 2996–2999.
[112] T. K. Ahn, K. S. Kim, D. Y. Kim, S. B. Noh, N. Aratani, C. Ikeda, A. Osuka, D. Kim, *J. Am. Chem. Soc.* **2006**, *128*, 1700–1704.
[113] G. W. Wheland, *Resonance in Organic Chemistry*, Wiley, New York, **1955**.
[114] M. G. Kuzyk, *J. Chem. Phys.* **2003**, *119*, 8327–8334.
[115] With a normalized TPA cross section (σ_2/N_c) of 124.5 for compound **31** (Table 2) and 126 for compound **C** of reference [77].
[116] D. F. Eaton, *J. Photochem. Photobiol. B* **1988**, *2*, 523–531.
[117] J. N. Demas, G. A. Crosby, *J. Phys. Chem.* **1971**, *75*, 991–1024.
[118] M. A. Albota, C. Xu, W. W. Webb, *Appl. Opt.* **1998**, *37*, 7352–7356.
[119] G. R. Pettit, M. P. Grealish, M. K. Jung, E. Hamel, R. K. Pettit, J.-C. Chapuis, J. M. Schmidt, *J. Med. Chem.* **2002**, *45*, 2534–2542.
[120] M. S. Wong, M. Samoc, A. Samoc, B. Luther-Davies, M. G. Humphrey, *J. Mater. Chem.* **1998**, *8*, 2005–2009.
[121] B. Tsuie, J. L. Reddinger, G. A. Sotzing, J. Soloducho, A. R. Katritzky, J. R. Reynolds, *J. Mater. Chem.* **1999**, *9*, 2189–2200.

Received: May 17, 2006
Published online: November 14, 2006

 © 2007 Wiley-VCH Verlag GmbH & Co. KGaA, Weinheim